

## MIT Open Access Articles

*Interval enclosures for reachable sets of chemical kinetic flow systems. Part 3: Indirect-bounding method*

The MIT Faculty has made this article openly available. **Please share** how this access benefits you. Your story matters.

**Citation:** Tulsyan, Aditya and Paul I. Barton. "Interval enclosures for reachable sets of chemical kinetic flow systems. Part 3: Indirect-bounding method." Chemical Engineering Science 166 (July 2017): 358-372 © 2017 Elsevier Ltd

**As Published:** <http://dx.doi.org/10.1016/J.CES.2017.02.047>

**Publisher:** Elsevier BV

**Persistent URL:** <https://hdl.handle.net/1721.1/128654>

**Version:** Author's final manuscript: final author's manuscript post peer review, without publisher's formatting or copy editing

**Terms of use:** Creative Commons Attribution-NonCommercial-NoDerivs License



# Interval enclosures for reachable sets of chemical kinetic flow systems. Part 3: indirect-bounding method

Aditya Tulsyan, Paul I. Barton

*Process Systems Engineering Laboratory, Massachusetts Institute of Technology, Cambridge, MA 02139, USA.*

---

## Abstract

In the third paper, in the three-part series, we propose an indirect-bounding approach for constructing rigorous interval enclosures or bounds for the reachable sets of CSTR reaction systems subject to parametric and initial condition uncertainties and flow rate disturbances. Existing comparison-based methods yield conservative enclosures for the reachable sets due to the non-quasi-monotonic and non-cooperative nature of CSTR reaction systems. The proposed indirect-bounding method addresses the overestimation problem by using the isomorphic transformation, developed in Tulsyan and Barton, 2016a [1], to map the system into a transformed state space, where comparison-based methods yield tight bounds. The interval bounds on the original states are then reconstructed using the inverse transformation. This eliminates the need to know a priori an effective enclosure set for the CSTR reaction system, as required by the direct-bounding method in Tulsyan and Barton, 2016b [2]. The efficacy of the indirect-bounding method is validated on several example problems. Several comparisons with the direct-bounding method are also presented to demonstrate the improvements achieved with the indirect-bounding method.

**Keywords:** Reaction kinetics; Reachable set; Transformation; Differential inequalities; and Interval arithmetic.

---

## 1. Introduction

The chemical reactions in a continuous stirred tank reactor (CSTR) are most often modeled by a set of continuous-time nonlinear ordinary differential equations (ODEs) that model the species concentrations in the CSTR as a function of the rate law and input-output flow rates. In this paper, we are interested in computing time-varying, component-wise rigorous bounds on the reachable sets of the species concentrations subject to various system uncertainties and flow rate disturbances. This is often referred to as the state enclosure or the state bounding problem. A short survey of the available methods to compute enclosures is provided next; however, for a detailed treatment on the subject, the readers are referred to Section 1 in [3], and the references cited therein.

In viability theory, the state enclosures are computed using the differential inclusion principle; wherein, the ODE system is expressed as an element of a set defined by the uncertain variables [4]. In contrast, comparison-based methods construct an auxiliary system whose solution is guaranteed to enclose the reachable set of the original system. A distinct advantage of comparison methods is that the auxiliary system does not rely on the uncertain variables; however, its performance does depend on the choice of the auxiliary system. One such comparison method applies the solutions of the Hamilton-Jacobi-Bellman and

Hamilton-Jacobi-Isaccs equations to enclose the reachable set [5, 6, 7]. Some recent work also applies the comparison principle by propagating geometries, such as polyhedrons [8, 9], zonotopes [10], ellipsoids [11], and their different combinations [12] forward in time to enclose the reachable set. Despite the rich literature, comparison-based methods incur higher computational cost. For example, solving the Hamilton-Jacobi equation involves numerical solution of a system of partial differential equations [7]. Furthermore, the complex geometries of these propagating objects does not offer easy handling and post-processing of enclosures in applications, such as optimization [13] and process monitoring [14] of high-dimensional systems.

A less expensive comparison principle applies differential inequalities to enclose the reachable set [15, 16]. Using differential inequalities, one can construct an auxiliary ODE system, whose solution is guaranteed to provide an interval enclosure of the reachable set. The primary advantage of the differential inequalities approach is that it can be implemented using interval arithmetic and numerical integration codes, thus yielding enclosures roughly at a cost comparable to a single simulation of the original system [17]. Despite the computational attractiveness of differential inequalities, there are several limitations of this approach – (1) its basic implementation is known to yield extremely conservative bounds for systems that are not quasi-monotone [15] or cooperative [18]. In [19], it was shown that many chemical processes of practical interest, including kinetic reaction systems, frequently violate these restrictive conditions. (2) The application of interval arithmetic and numerical integration codes contributes to over-

---

<sup>\*</sup>Corresponding author P. I. Barton.

Email addresses: [tulsyan@mit.edu](mailto:tulsyan@mit.edu) (Aditya Tulsyan),  
[pib@mit.edu](mailto:pib@mit.edu) (Paul I. Barton)

estimation of the enclosure. This is due to the dependency problem and wrapping effect, inherent with the application of interval methods [20]. Further, although not significant, the use of non-verified numerical integration methods can result in overestimation, and for certain systems, may even yield invalid bounds. This problem can be mitigated by using modern numerical integration schemes or other computationally involved hybrid formulations [21].

To leverage the low computational cost of differential inequalities, much work has been done to address the overestimation issue. In [19], it was shown that for certain well-understood systems, it is often possible to construct a priori a set  $G_x$ , which is guaranteed to enclose the reachable set of the system. Using an a priori enclosure set  $G_x$ , a generalized differential inequalities method was proposed in [17] to compute tighter and improved bounds on the system. The efficacy of the generalized method for CSTR reaction systems (or direct-bounding method) is discussed in the second paper [2]; wherein an a priori enclosure for the system is computed using the transformation proposed in the first paper [1]. Despite the success with the direct-bounding method, identifying a tight a priori enclosure set,  $G_x$  for many practical systems of interest is challenging and time-consuming. Furthermore, as shown in [2], the degree of overestimation with the direct-bounding method depends on the set  $G_x$ .

In this paper, we propose an indirect-bounding method to compute efficient interval enclosures for the reachable sets of CSTR reaction systems. Instead of bounding the original CSTR reaction system – for which a nontrivial a priori enclosure is not available or too difficult to compute – the indirect-bounding method uses the isomorphic transformation developed in [1] to map the system into a transformed state space, where it is relatively easier to bound using the generalized differential inequalities. The enclosure for the original CSTR system is then computed using the inverse transformation. This completely eliminates the need to know a priori an enclosure for the CSTR system in the original state space. The indirect-bounding method is computationally fast, since enclosure computation in the transformed space is much easier than in the original state space. Further, the sparse property of the transformation in [1] also significantly minimizes the wrapping effect, dependency problem, and other numerical errors, including the integration errors. Finally, the efficacy of the proposed indirect-bounding method is demonstrated on example problems.

It is instructive to highlight that both direct and indirect bounding methods make use of the transformation developed in [2] to compute enclosures for the CSTR reaction system; however, there is a significant difference in the way the transformation is used. While the indirect-bounding method applies the transformation to map the system into the transformed state space, the direct-bounding method applies the transformation to provide an efficient a priori enclosure for the system in the original state space. This constitutes the basic difference between the indirect and

direct methods in terms of their design. Other differences between the direct and indirect bounding methods are discussed in details in Section 5. The notation used in this paper is discussed next along with a brief introduction to interval arithmetic.

**Notation.** Lower-case and upper-case bold letters denote vectors and matrices, respectively.  $\mathbf{v}^T$  (or  $\mathbf{M}^T$ ) denotes the transpose of a vector (or matrix).  $\mathbf{0}_{m \times n}$  and  $\mathbf{1}_{m \times n}$  will denote  $m \times n$  matrices of zeros and ones, respectively, and  $\mathbf{I}_n$  an  $n \times n$  identity matrix. For  $\mathbf{A} \in \mathbb{R}^{m \times n}$ , the rank of the matrix is denoted by  $\text{Rank}(\mathbf{A})$  and the null space as  $\mathcal{N}(\mathbf{A}) = \{\mathbf{x} \in \mathbb{R}^n : \mathbf{A}\mathbf{x} = \mathbf{0}_{m \times 1}\}$ . For every finite, real matrix  $\mathbf{A} \in \mathbb{R}^{m \times n}$ , let  $\mathbf{A}^+ \in \mathbb{R}^{n \times m}$  denote its Moore-Penrose inverse. Vector equality/inequality is to be understood component-wise. For two vectors  $\mathbf{x}^L, \mathbf{x}^U \in \mathbb{R}^n$  satisfying  $\mathbf{x}^L \leq \mathbf{x}^U$ ,  $X \equiv [\mathbf{x}^L, \mathbf{x}^U] \equiv [x_1^L, x_1^U] \times [x_2^L, x_2^U] \times \cdots \times [x_n^L, x_n^U]$  denotes an  $n$ -dimensional interval in  $\mathbb{R}^n$ . The set of nonempty compact intervals in  $\mathbb{R}^n$  is denoted by  $\mathbb{IR}^n$ .  $X$  is negative if  $\mathbf{x} < \mathbf{0}_n$  for all  $\mathbf{x} \in X$  and degenerate if  $\mathbf{x}^L = \mathbf{x}^U$ . Positive intervals are defined likewise.  $\mathbb{R}_+$  denotes the set of non-negative reals. For  $n \in \mathbb{N}$  and any measurable set  $T \subset \mathbb{R}$ , the space of Lebesgue integrable functions  $\mathbf{v} : T \rightarrow \mathbb{R}^n$  is denoted by  $L^1(T, \mathbb{R}^n) \equiv \{(\mathbf{v} : T \rightarrow \mathbb{R}^n) : \int_T |\mathbf{v}_i| < +\infty, \forall i\}$ , such that  $\mathbf{v} \in L^1(T, \mathbb{R}^n)$  implies  $v_i \in L^1(T, \mathbb{R})$  for all  $i$ .

**Interval Arithmetic.** Interval arithmetic [20] is a powerful method that provides means to enclose the range of a function on an interval. For  $E \subset \mathbb{R}^n$ , let  $\mathbb{I}E$  denote the interval set  $\{Z \in \mathbb{IR}^n | Z \subset E\}$ . If  $\mathbf{f} : E \rightarrow \mathbb{R}^m$  is a function of interest, then the mapping  $[\mathbf{f}] : \mathbb{I}E \rightarrow \mathbb{IR}^m$  is called an interval extension of  $\mathbf{f}$  on  $E$ , if the equality

$$[\mathbf{f}]([\mathbf{y}, \mathbf{y}]) = [\mathbf{f}(\mathbf{y}), \mathbf{f}(\mathbf{y})], \quad \forall \mathbf{y} \in E,$$

holds for all degenerate intervals (singletons).  $[\mathbf{f}]$  is inclusion monotonic on  $E$ , if for any two intervals  $Y, Y' \in \mathbb{I}E$ ,

$$Y \subset Y' \implies [\mathbf{f}](Y) \subset [\mathbf{f}](Y').$$

Finally, it can be shown [20] that an inclusion monotonic interval extension of  $\mathbf{f}$  always encloses its range, such that

$$\mathbf{f}(X) \subset [\mathbf{f}](X), \quad \forall X \in \mathbb{I}E,$$

where  $\mathbf{f}(X)$  is the image or reachable set of  $X$  under  $\mathbf{f}$ .

## 2. CSTR Reaction Model

Let  $n_x \in \mathbb{N}$  denote the number of species,  $n_r \in \mathbb{N}$  the number of chemical reactions,  $n_k \in \mathbb{N}$  the number of uncertain rate-constants and  $n_p \in \mathbb{N}$  the number of input flow rates in a chemical kinetic system. For mathematical convenience, the CSTR is assumed to have one outlet; however, this need not be the case, in general. For given compact sets  $D_k \subset \mathbb{R}^{n_k}$ ,  $D_{u_i} \subset \mathbb{R}^{n_p}$  and  $D_{u_o} \subset \mathbb{R}$ , let  $\mathbf{k}(t) \in D_k$  be the time-varying uncertain parameters (also includes

time-invariant parameters),  $\mathbf{u}_i(t) \in D_{u_i}$  be the input flow rates and  $u_o(t) \in D_{u_o}$  denote the output flow rates. Defining  $\mathbf{u}(t) \equiv (\mathbf{k}(t), \mathbf{u}_i(t), u_o(t)) \in U \equiv D_k \times D_{u_i} \times D_{u_o}$ , let the set of time-varying inputs/parameters be denoted in a compact notation as

$$\mathcal{U} = \{\mathbf{u} \in L^1(T, \mathbb{R}^{n_k+n_p+1}) : \mathbf{u}(t) \in U, \text{ a.e. } t \in T\},$$

where  $T = [t_0, t_f] \subset \mathbb{R}$  is some time interval of interest. For a given set  $D_x \subset \mathbb{R}^{n_x}$ , let the set of initial concentrations of the species in the CSTR at  $t_0$  be  $X_0 \subset D_x$ . Let  $\mathbf{S} \in \mathbb{R}^{n_x \times n_r}$  and  $\mathbf{W} \in \mathbb{R}^{n_x \times n_p}$  be the stoichiometric and volumetric concentration matrices, respectively. Finally, for a rate function  $\mathbf{r} : T \times D_k \times D_x \rightarrow \mathbb{R}^{n_x}$ , the concentration profile of species in a CSTR of constant volume  $V \in \mathbb{R}_+$  can be modeled as an IVP given by

$$\dot{\mathbf{x}}(t, \mathbf{u}) = \mathbf{S}\mathbf{r}(\mathbf{k}(t), \mathbf{x}(t, \mathbf{u})) + \frac{1}{V}\mathbf{W}\mathbf{u}_i(t) - \frac{u_o(t)}{V}\mathbf{x}(t, \mathbf{u}), \quad (1)$$

with  $\mathbf{x}(t_0, \mathbf{u}) \in X_0$ . In (1), the outlet flow depends on the inlet flow such that

$$u_o(t) = \mathbf{1}_{n_p \times 1}^T \mathbf{u}_i(t), \quad (2)$$

holds for all  $\mathbf{u}_i(t) \in D_{u_i}$  and at every  $t \in T$ . The solution to the IVP (1) is defined as a mapping  $\mathbf{x} : T \times \mathcal{U} \rightarrow D_x$  such that for each  $\mathbf{u} \in \mathcal{U}$ ,  $\mathbf{x}(\cdot, \mathbf{u})$  is absolutely continuous and satisfies (1) a.e. on  $T$ . We assume that for each  $(\mathbf{u}, \mathbf{x}_0) \in \mathcal{U} \times X_0$ , a unique solution to (1) exists on a given time horizon  $T$ .

**Problem Statement.** Given interval sets  $U$ ,  $X_0$ , and  $T$ , compute enclosures of the form  $[\mathbf{x}] \equiv [\mathbf{x}^L, \mathbf{x}^U]$  for the CSTR reaction system in (1), such that for the two continuous functions  $\mathbf{x}^L, \mathbf{x}^U : T \rightarrow \mathbb{R}^{n_x}$ ,  $\mathbf{x}(t, \mathbf{u}) \in [\mathbf{x}^L(t), \mathbf{x}^U(t)]$ , for each  $(\mathbf{u}, \mathbf{x}_0) \in \mathcal{U} \times X_0$  and for all  $t \in T$ .

### 3. Generalized Differential Inequalities

In this section, we briefly discuss the generalized differential inequalities approach developed in [17] for computing interval enclosures for nonlinear ODE systems with  $L^1(T)$  control inputs. The discussion in this section is strictly limited to its application in the indirect-bounding method proposed in Section 4; however, for a more general discussion on the generalized differential inequalities, the readers are referred to the original paper [17], or an abridged version discussed in Section 3 in [2].

Let  $\mathbf{f} : T \times U \times D_x \rightarrow \mathbb{R}^{n_x}$  denote a generic right-hand side function of an IVP, which for (1) is defined as

$$\mathbf{f}(t, \mathbf{u}(t), \mathbf{x}(t, \mathbf{u})) \equiv \mathbf{S}\mathbf{r}(\mathbf{k}(t), \mathbf{x}(t, \mathbf{u})) + \frac{1}{V}\mathbf{W}\mathbf{u}_i(t) - \frac{u_o(t)}{V}\mathbf{x}(t, \mathbf{u}),$$

then the theory of generalized differential inequalities as proposed in [17] is given by

**Theorem 1** (Th. 2 in [17]). For  $D_\Omega \subset \mathbb{R}^{n_x} \times \mathbb{R}^{n_x}$ , let  $\Omega_i^L, \Omega_i^U : D_\Omega \rightarrow \mathbb{I}\mathbb{R}^{n_x}$  for  $i = 1, \dots, n_x$  be set-valued mappings satisfying Assumption 3 in [17] and let  $\mathbf{x}^L, \mathbf{x}^U : T \rightarrow \mathbb{R}^{n_x}$  be absolutely continuous functions satisfying

1. For every  $t \in T$  and every index  $i$ 
  - (a)  $(\mathbf{x}^L(t), \mathbf{x}^U(t)) \in D_\Omega$ ,
  - (b)  $\Omega_i^L(\mathbf{x}^L(t), \mathbf{x}^U(t)) \subset D_x$  and  $\Omega_i^U(\mathbf{x}^L(t), \mathbf{x}^U(t)) \subset D_x$ .
2.  $X_0 \subset [\mathbf{x}^L(t_0), \mathbf{x}^U(t_0)]$ .
3. For a.e.  $t \in T$  and every index  $i$ 
  - (a)  $\dot{\mathbf{x}}_i^L(t) \leq f_i(t, \mathbf{p}, \mathbf{g}), \forall \mathbf{g} \in \Omega_i^L(\mathbf{x}^L(t), \mathbf{x}^U(t)), \mathbf{p} \in U$ ,
  - (b)  $\dot{\mathbf{x}}_i^U(t) \geq f_i(t, \mathbf{p}, \mathbf{g}), \forall \mathbf{g} \in \Omega_i^U(\mathbf{x}^L(t), \mathbf{x}^U(t)), \mathbf{p} \in U$ .

Then  $\mathbf{x}(t, \mathbf{u}) \in [\mathbf{x}^L(t), \mathbf{x}^U(t)]$  for each  $(\mathbf{u}, \mathbf{x}_0) \in \mathcal{U} \times X_0$  and for all  $t \in T$ .

In Theorem 1,  $D_\Omega$ ,  $\Omega_i^L$ , and  $\Omega_i^U$  are user-defined objects which need to be designed a priori. The two designs proposed in [17], and discussed in Section 3.1 in [2] are:

- (a) Consider Theorem 1 with:

$$\begin{aligned} D_\Omega &\equiv \{(\mathbf{x}^L, \mathbf{x}^U) \in \mathbb{R}^{n_x} \times \mathbb{R}^{n_x} : \mathbf{x}^L \leq \mathbf{x}^U\}, \\ \Omega_i^L(\mathbf{x}^L, \mathbf{x}^U) &\equiv \mathcal{F}_i^L([\mathbf{x}^L, \mathbf{x}^U]), \\ \Omega_i^U(\mathbf{x}^L, \mathbf{x}^U) &\equiv \mathcal{F}_i^U([\mathbf{x}^L, \mathbf{x}^U]), \end{aligned} \quad (3)$$

for every  $i = 1, \dots, n_x$ . Here  $\mathcal{F}_i^L, \mathcal{F}_i^U : \mathbb{I}\mathbb{R}^{n_x} \rightarrow \mathbb{I}\mathbb{R}^{n_x}$  are interval-valued mappings in Definition 1 in [2].

- (b) Consider Theorem 1 with:

$$\begin{aligned} D_\Omega &\equiv \{(\mathbf{x}^L, \mathbf{x}^U) \in \mathbb{R}^{n_x} \times \mathbb{R}^{n_x} : [\mathbf{x}^L, \mathbf{x}^U] \in D_{\mathcal{P}}\}, \\ \Omega_i^L(\mathbf{x}^L, \mathbf{x}^U) &\equiv \mathcal{F}_i^L(\mathcal{P}_{G_x}[\mathbf{x}^L, \mathbf{x}^U]), \\ \Omega_i^U(\mathbf{x}^L, \mathbf{x}^U) &\equiv \mathcal{F}_i^U(\mathcal{P}_{G_x}[\mathbf{x}^L, \mathbf{x}^U]), \end{aligned} \quad (4)$$

for every  $i = 1, \dots, n_x$ . Here, for  $D_{\mathcal{P}} \subset \mathbb{I}\mathbb{R}^{n_x}$ ,  $\mathcal{P}_{G_x} : D_{\mathcal{P}} \rightarrow \mathbb{I}\mathbb{R}^{n_x}$  is a Lipschitz interval-valued mapping as defined in Definition 2 in [2], and  $G_x : T \rightarrow \mathbb{R}^{n_x}$  is an a priori set containing the reachable set of  $\mathbf{x}(t, \mathbf{u}) \in G_x(t)$  for each  $(\mathbf{x}_0, \mathbf{u}) \in X_0 \times \mathcal{U}$  and for all  $t \in T$ .

Interval arithmetic provides an efficient way to implement Theorem 1. Interval implementation of Theorem 1 involves evaluating a natural interval extension of  $\mathbf{f}$  over the sets described in Hypothesis 3. Using interval arithmetic, we obtain the following (see [17, 2] for details)

$$\begin{aligned} \dot{\mathbf{x}}_i^L(t) &= f_i^L([t, t], U, \Omega_i^L(\mathbf{x}^L(t), \mathbf{x}^U(t))), \\ \dot{\mathbf{x}}_i^U(t) &= f_i^U([t, t], U, \Omega_i^U(\mathbf{x}^L(t), \mathbf{x}^U(t))), \end{aligned} \quad (5)$$

where  $[f_i] \equiv [f_i^L, f_i^U]$  is a natural interval extension of  $\mathbf{f}$  and  $[\mathbf{x}_i^L(t_0), \mathbf{x}_i^U(t_0)] \supset X_{0,i}$  holds for every  $i = 1, \dots, n_x$ .

Finally, if  $(\mathbf{x}^L, \mathbf{x}^U)$  are absolutely continuous functions satisfying (5) a.e. on  $T$ , then  $\mathbf{x}(t, \mathbf{u}) \in [\mathbf{x}^L(t), \mathbf{x}^U(t)]$  for each  $(\mathbf{u}, \mathbf{x}_0) \in \mathcal{U} \times X_0$  and for all  $t \in T$  (see Corollary 3 in [17]). In other words, integrating the IVP in (5) yields the required time-varying, component-wise interval enclosure for the reachable set of a CSTR reaction system in (1). Note that (5) holds with either (3) or (4).

### 3.1. Overestimation with Theorem 1

The main source of overestimation in the implementation of Theorem 1 with (3) or (4) is the application of interval methods to construct (5). This is further exacerbated due to the non-quasi-monotonic and non-cooperative nature of the CSTR reaction system in (1). Even though solving Theorem 1 with (4) is more effective (as compared to solving it with (3)) at reducing conservatism through the use of an a priori enclosure set  $G_x$ , overestimation issues with the implementation of Theorem 1 still persist.

The degree of conservatism in implementing Theorem 1 depends on the quality of  $[\mathbf{f}]$  computed in (5). Ideally,  $[\mathbf{f}]$  should exactly map to the image of the input set under  $\mathbf{f}$ ; however, this is rarely true, unless  $\mathbf{f}$  belongs to a class of intrinsic functions (e.g.,  $\sin$ ,  $\exp$ ) [20]. For all other functions, overestimation with interval methods is almost always systematic due to the wrapping effect and dependency problem [20]. The wrapping effect is a result of the actual arbitrary-shaped image set being wrapped by an interval enclosure. In general, the wrapping effect is significant in nonlinear multivariate functions, whose image sets are not necessarily intervals. Further, the overestimation due to the dependency problem arises from the inability of interval analysis to recognize multiple occurrences of the same variable in a given function. For example, if  $f(x) = x - x$  for all  $x \in X$ , where  $X = [-1, 2]$  then an interval extension of  $f$  over  $X$  is  $[f](X) = [-1, 2] - [-1, 2] = [-3, 3]$ , while the actual image of  $X$  under the function,  $f(X)$  is  $[0, 0]$ .

In (5), since  $[\mathbf{f}]$  computed at the current time uses intervals from the previous time instants, any existing conservatism in  $[\mathbf{x}^L, \mathbf{x}^U]$  is fed back, and eventually builds-up as (5) is integrated forward in time. This is referred to as the conservatism build-up with Theorem 1. The conservatism build-up has been observed in many systems, including batch reactors [19, 22]. In [19, 22] it was shown that Theorem 1 with (3) results in extremely large upper bounds after a short integration time, and for some species, the bounds tend towards infinity. Later, [17] showed that implementing Theorem 1 with (4) yields a much tighter enclosure from the use of  $G_x$ . Nevertheless, as shown in [2], given (1), the degree of conservatism with (4) is contingent on the quality of the a priori set  $G_x$ .

Despite the success in computing enclosures for batch reaction systems using Theorem 1, designing an a priori set  $G_x$  for many practical systems, including (1) is challenging and time-consuming. Despite the effort made in [2], the design of  $G_x$  is still non-unique and open, and at present, it is not immediately clear what is the ideal design for  $G_x$  that yields the tightest interval enclosure for (1). In other words, the conservatism with the “direct” implementation of Theorem 1 is conditioned on knowing a tight a priori enclosure  $G_x$ .

To address the limitation of knowing a priori, an efficient design for  $G_x$ , and to address the overestimation issues inherent with the implementation of Theorem 1, we

propose an indirect-bounding method to compute enclosures for CSTR reaction systems. The indirect method is discussed in the next section.

## 4. Indirect Bounding Method

In this section, we present a novel approach to compute efficient state enclosures for the reachable sets of CSTR reaction systems. As discussed in Section 3.1, any direct implementation of Theorem 1 to compute bounds for (1) is inefficient due to the lack of a tight a priori enclosure design, and subsequent mechanisms to deal with the interval arithmetic-related overestimation issues. To address these problems, an indirect-bounding method is proposed in this paper. The central idea is the use of the isomorphic transformation in [1] to map the reachable set  $\mathbf{x}(t, \mathcal{U})$  into a transformed state space  $\mathbf{z}(t, \mathcal{U})$ . In the transformed space, an enclosure for  $\mathbf{z}(t, \mathcal{U})$  is computed using Theorem 1, which is finally “inverted” using the inverse transformation to compute enclosures for  $\mathbf{x}(t, \mathcal{U})$ . Now, since the state enclosure for  $\mathbf{x}(\cdot, \mathcal{U})$  is computed indirectly, using the bounding results available for  $\mathbf{z}(\cdot, \mathcal{U})$ , this approach is called an indirect-bounding method. The schematic of the indirect-bounding method is given in Figure 1. As shown in Figure 1, the indirect-bounding method can be decomposed into the following key steps:

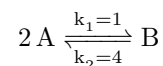
1. transforming the CSTR reaction system;
2. enclosure in transformed state space; and
3. reconstructing the enclosure in the original state space.

The aforementioned steps are nontrivial, and are further discussed next in Sections 4.1 through 4.3.

### 4.1. Step 1: Transformation

The first step involves mapping the dynamics of the CSTR reaction system in (1) into a transformed state space. Apart from the transformation being isomorphic (or invertible), which is necessary for recovering the enclosures in the original state space, the reachable set of the system in the transformed state space should also be relatively easier to bound (as compared to computing bounds in the original state space) using Theorem 1. Using similar arguments presented in Section 3.1, for Theorem 1 to be effective, the wrapping effect and dependency problem in the transformed state space should be minimized. As discussed in [2], overestimation in bounding (1) arises due to the matrices  $\mathbf{S}$  and  $\mathbf{W}$ . This is because multiplying  $\mathbf{r}$  and  $\mathbf{u}_i$  with possibly dense matrices  $\mathbf{S}$  and  $\mathbf{W}$ , respectively, introduces dependency between the uncertain variables. This is illustrated in the example below.

**Example 1.** Consider the following reversible reaction



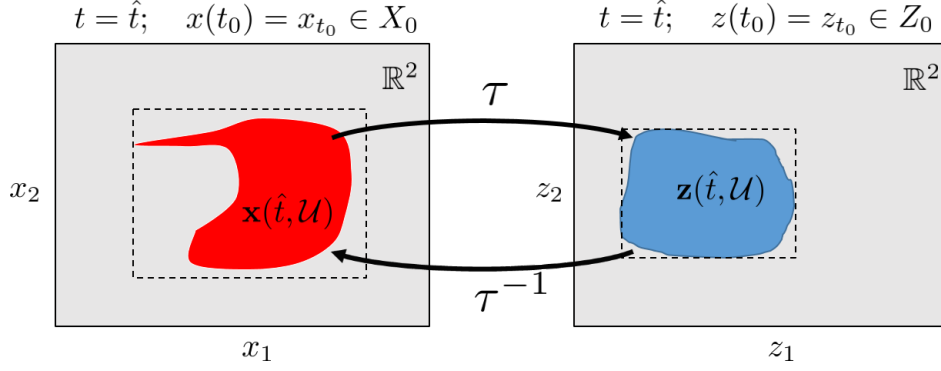


Figure 1: An illustration of the indirect-bounding method. The original solution set, denoted by  $\mathbf{x}(\hat{t}, \mathcal{U})$ , is first transformed to the set  $\mathbf{z}(\hat{t}, \mathcal{U})$  using an isomorphic transformation, denoted generically by  $\tau$ . Bounds on the transformed solution set  $\mathbf{z}(\hat{t}, \mathcal{U})$  are computed using Theorem 1, and filtered through  $\tau^{-1}$  to recover bounds on the original solution set.

in a CSTR of unit volume with 2 inlet flow streams  $\mathbf{u}_i(t) = [u_{i,1}(t) \ u_{i,2}(t)]^T$  and one outlet  $u_o(t) = u_{i,1}(t) + u_{i,2}(t)$ . The stream  $u_{i,1}$  contains 1M of species A and B, while  $u_{i,2}$  contains 2M of A and B. The initial concentrations for A and B are 1M each. Assuming mass-action kinetic law, the dynamics in the reactor are modeled as

$$\begin{aligned} \dot{\mathbf{x}}(t, \mathbf{u}) &= \begin{bmatrix} -2 & 2 \\ 1 & -1 \end{bmatrix} \begin{bmatrix} x_A^2 \\ 4x_B \end{bmatrix} + \begin{bmatrix} 1 & 2 \\ 1 & 2 \end{bmatrix} \mathbf{u}_i(t) \\ &\quad - u_o(t)\mathbf{x}(t, \mathbf{u}), \\ \mathbf{x}(0) &= \mathbf{1}_{2 \times 1}. \end{aligned}$$

For the given  $\mathbf{S}$  and  $\mathbf{W}$ , the state derivative,  $\dot{\mathbf{x}}$ , is a complex nonlinear function of the states and input flow rates. Contrast this with the case when  $\mathbf{S}$  and  $\mathbf{W}$  are replaced with identity matrices, for example. Computing bounds for (1) with dense  $\mathbf{S}$  and  $\mathbf{W}$  matrices not only make the dependency problem pronounced with the application of interval-based methods, the wrapping effect is also amplified due to the complex reaction dynamics. Thus as a general rule, the “simpler” the right-hand-side function in (1), the more effective Theorem 1 is in generating tight enclosures for the reachable set.

In order to obtain tight enclosures with Theorem 1, we require a “sparse” representation of the CSTR reaction system in the transformed state space. Typically, this can be achieved by using a transformation that replaces  $\mathbf{S}$  and  $\mathbf{W}$  with sparse matrices. This was explored in the first paper [1]. For the sake of brevity, only the main result is presented next; however, a detailed treatment involving development of the sparse transformation can be found in [1].

**Theorem 2** (Th. 2 in [1]). Consider the CSTR reaction system in (1) under the following hypotheses:

1.  $\text{Rank}(\mathbf{S}) = n_r$ ;
2.  $\text{Rank}(\mathbf{W}) = n_p$ ;
3.  $n_x > n_r + n_p$ ; and

$$4. \text{Rank}(\mathbf{N}^T \mathbf{W}) = n_p.$$

Given  $\mathbf{S}$ , let  $\mathbf{S}^+ \in \mathbb{R}^{n_r \times n_x}$  be its Moore-Penrose inverse and  $\mathbf{N} \in \mathbb{R}^{n_x \times (n_x - n_r)}$  be a basis for  $\mathcal{N}(\mathbf{S}^T)$ . Given  $\mathbf{N}^T \mathbf{W}$ , let  $\mathbf{M}^+ \in \mathbb{R}^{n_p \times (n_x - n_r)}$  be its Moore-Penrose inverse and  $\mathbf{F} \in \mathbb{R}^{(n_x - n_r) \times (n_x - n_r - n_p)}$  be a basis for  $\mathcal{N}(\mathbf{W}^T \mathbf{N})$ , then there exists a unique solution to

$$\dot{\mathbf{z}}_1(t, \mathbf{u}) = -\frac{u_o(t)}{V} \mathbf{z}_1(t, \mathbf{u}), \quad (6a)$$

$$\dot{\mathbf{z}}_2(t, \mathbf{u}) = \frac{1}{V} \mathbf{u}_i(t) - \frac{u_o(t)}{V} \mathbf{z}_2(t, \mathbf{u}), \quad (6b)$$

$$\begin{aligned} \dot{\mathbf{z}}_3(t, \mathbf{u}) &= \mathbf{r}(\mathbf{k}(t), \mathbf{S} \mathbf{z}_3(t, \mathbf{u}) + \mathbf{W} \mathbf{z}_2(t, \mathbf{u}) \\ &\quad + \mathbf{N}(\mathbf{N}^T \mathbf{N})^{-1} \mathbf{F}(\mathbf{F}^T \mathbf{F})^{-1} \mathbf{z}_1(t, \mathbf{u})) - \frac{u_o(t)}{V} \mathbf{z}_3(t, \mathbf{u}), \end{aligned} \quad (6c)$$

satisfying the conditions

$$\mathbf{z}(t, \mathbf{u}) \equiv \begin{bmatrix} \mathbf{z}_1(t, \mathbf{u}) \\ \mathbf{z}_2(t, \mathbf{u}) \\ \mathbf{z}_3(t, \mathbf{u}) \end{bmatrix} = \begin{bmatrix} \mathbf{F}^T \mathbf{N}^T \\ \mathbf{M}^+ \mathbf{N}^T \\ \mathbf{S}^+ (\mathbf{I}_{n_x} - \mathbf{W} \mathbf{M}^+ \mathbf{N}^T) \end{bmatrix} \mathbf{x}(t, \mathbf{u}), \quad (7a)$$

$$\begin{aligned} \mathbf{x}(t, \mathbf{u}) &= \mathbf{S} \mathbf{z}_3(t, \mathbf{u}) + \mathbf{W} \mathbf{z}_2(t, \mathbf{u}) \\ &\quad + \mathbf{N}(\mathbf{N}^T \mathbf{N})^{-1} \mathbf{F}(\mathbf{F}^T \mathbf{F})^{-1} \mathbf{z}_1(t, \mathbf{u}), \end{aligned} \quad (7b)$$

for all  $(t, \mathbf{u}, \mathbf{x}_0) \in T \times \mathcal{U} \times X_0$ .

Theorem 2 does not make any explicit assumptions on the rate function or the flow rates. In other words, Theorem 2 is general, and applicable to a wide class of CSTR systems and under different flow conditions. The IVP (6a) – (6c) is the sparsest representation of (1) in the transformed state space. From the bounding perspective, the sparsity in the IVP (6a) – (6c) minimizes the dependency between uncertain variables. In Section 4.2, we show that enclosure for the reachable set of the IVP (6a) – (6c) are also relatively simpler to calculate. This is discussed in the next section.

#### 4.2. Step 2: Bounding

In this section, we discuss the procedure for computing enclosures for the reachable set of  $\mathbf{z}$  generated by the IVP

in Theorem 2 using the theory of generalized differential inequalities outlined in Theorem 1. This constitutes Step 2 of the indirect-bounding method discussed in Section 4. Note that this step is also explored in the second paper [2] as a part of the direct-bounding method. For the sake of completeness, key results from [2] are revisited to highlight the procedure to compute enclosures for the reachable set of  $\mathbf{z}$ .

#### 4.2.1. Bounding State $\mathbf{z}_1$

In Theorem 2, since  $\mathbf{z}_1$  is independent of  $\mathbf{z}_2$  and  $\mathbf{z}_3$ , state  $\mathbf{z}_1$  can be described by the following independent IVP

$$\dot{\mathbf{z}}_1(t, \mathbf{u}) = -\frac{u_o(t)}{V}\mathbf{z}_1(t, \mathbf{u}), \quad (8)$$

with  $\mathbf{z}_1(t_0, \mathbf{u}) \in Z_{1,0} \subset \mathbb{R}^{n_x - n_r - n_p}$ , where

$$Z_{1,0} \equiv [\mathbf{z}_{1,0}^L, \mathbf{z}_{1,0}^U] = \mathbf{F}^T \mathbf{N}^T [\mathbf{x}_0^L, \mathbf{x}_0^U]. \quad (9)$$

Given (8) and sets  $U$ ,  $Z_{1,0}$  and  $T$ , let  $[\mathbf{z}_1] \equiv [\mathbf{z}_1^L, \mathbf{z}_1^U]$  represent a valid bound for  $\mathbf{z}_1$  such that

$$\mathbf{z}_1^L(t) \leq \mathbf{z}_1(t, \mathbf{u}) \leq \mathbf{z}_1^U(t), \quad (10)$$

holds for each  $(\mathbf{u}, \mathbf{z}_{1,0}) \in \mathcal{U} \times Z_{1,0}$  and for all  $t \in T$ . Here,  $\mathbf{z}_1^L$  and  $\mathbf{z}_1^U$  can be computed using the theory of generalized differential inequalities outlined in Theorem 1. Alternatively, in certain special cases, it is also possible to compute bounds for (8) using just the interval extensions. First observe that if for each  $(\mathbf{u}, \mathbf{z}_{1,0}) \in \mathcal{U} \times Z_{1,0}$ , the output flow rate is restricted to a class of uncertain constant functions, i.e.  $u_o(t) = u_o \in D_{u_o}$  for all  $t \in T$ , then the IVP in (8) exhibits an analytic solution over  $t \in T$  given by

$$\mathbf{z}_1(t, \mathbf{u}) = \mathbf{z}_1(t_0, \mathbf{u}) \exp\left(-\frac{u_o}{V}t\right). \quad (11)$$

Evaluating the natural interval extension of (11) over  $U$  and  $Z_{1,0}$  yields

$$[\mathbf{z}_1^L(t), \mathbf{z}_1^U(t)] = [\mathbf{z}_{1,0}^L, \mathbf{z}_{1,0}^U] \exp\left(-\frac{[u_o^L, u_o^U]}{V}t\right), \quad (12)$$

for all  $t \in T$ . Now, since the interval extension of a monotonic intrinsic function is the exact range of the function [20], the bounds in (12) are the same as the range of (11) over the sets  $U$  and  $Z_{1,0}$ .

#### 4.2.2. Bounding State $\mathbf{z}_2$

As in Section 4.2.1,  $\mathbf{z}_2$  is independent of  $\mathbf{z}_1$  and  $\mathbf{z}_3$ , such that the IVP for  $\mathbf{z}_2$  can be written as

$$\dot{\mathbf{z}}_2(t, \mathbf{u}) = \frac{1}{V}\mathbf{u}_i(t) - \frac{u_o(t)}{V}\mathbf{z}_2(t, \mathbf{u}), \quad (13)$$

with  $\mathbf{z}_2(t_0, \mathbf{u}) \in Z_{2,0} \subset \mathbb{R}^{n_p}$ , where

$$Z_{2,0} \equiv [\mathbf{z}_{2,0}^L, \mathbf{z}_{2,0}^U] = \mathbf{M}^+ \mathbf{N}^T [\mathbf{x}_0^L, \mathbf{x}_0^U]. \quad (14)$$

As previously, Theorem 1 can be applied to bound  $\mathbf{z}_2$ ; however, if input flow rates are restricted to a class of uncertain constant functions, i.e.,  $\mathbf{u}_i(t) = \mathbf{u}_i \in D_{u_i}$ , then the output flow rate is also constant from (2). Setting  $u_o(t) = u_o \in D_{u_o}$  for all  $t \in T$ , for each  $(\mathbf{u}, \mathbf{z}_{2,0}) \in \mathcal{U} \times Z_{2,0}$ , the IVP in (13) has a closed-form solution given by

$$\mathbf{z}_2(t, \mathbf{u}) = \mathbf{z}_2(t_0, \mathbf{u}) \exp\left(-\frac{u_o}{V}t\right) + \frac{\mathbf{u}_i}{u_o}\left(1 - \exp\left(-\frac{u_o}{V}t\right)\right). \quad (15)$$

Given (15) and sets  $U$ ,  $Z_{2,0}$  and  $T$ , the interval extension of (15) is given by

$$[\mathbf{z}_2^L(t), \mathbf{z}_2^U(t)] = [\mathbf{z}_{2,0}^L, \mathbf{z}_{2,0}^U] \exp\left(-\frac{[u_o^L, u_o^U]}{V}t\right) + \frac{[\mathbf{u}_i^L, \mathbf{u}_i^U]}{[u_o^L, u_o^U]} \times \left(1 - \exp\left(-\frac{[u_o^L, u_o^U]}{V}t\right)\right). \quad (16)$$

where  $[\mathbf{z}_2] \equiv [\mathbf{z}_2^L, \mathbf{z}_2^U]$  satisfies

$$\mathbf{z}_2^L(t) \leq \mathbf{z}_2(t, \mathbf{u}) \leq \mathbf{z}_2^U(t), \quad (17)$$

for each  $(\mathbf{u}, \mathbf{z}_{2,0}) \in \mathcal{U} \times Z_{2,0}$  and for all  $t \in T$ . Further, note that the dependency problem in (16) manifests only for the multi-input case, i.e., for  $n_p > 1$ . For  $n_p = 1$ , since  $u_i = u_o$ , (15) can be simplified and written as

$$\mathbf{z}_2(t, \mathbf{u}) = \mathbf{z}_2(t_0, \mathbf{u}) \exp\left(-\frac{u_o}{V}t\right) + \left(1 - \exp\left(-\frac{u_o}{V}t\right)\right), \quad (18)$$

and its interval extension as

$$[\mathbf{z}_2^L(t), \mathbf{z}_2^U(t)] = [\mathbf{z}_{2,0}^L, \mathbf{z}_{2,0}^U] \exp\left(-\frac{[u_o^L, u_o^U]}{V}t\right) + \left(1 - \exp\left(-\frac{[u_o^L, u_o^U]}{V}t\right)\right). \quad (19)$$

Since the flow rates pre-multiplying the second term are removed, (19) provides an exact, closed-form bounding solution for  $\mathbf{z}_2$ .

#### 4.2.3. Bounding State $\mathbf{z}_3$

The IVP for the transformed state  $\mathbf{z}_3$  in (6c) is given by

$$\dot{\mathbf{z}}_3(t, \mathbf{u}) = \mathbf{r}\left(\mathbf{k}(t), \mathbf{S}\mathbf{z}_3(t, \mathbf{u}) + \mathbf{W}\mathbf{z}_2(t, \mathbf{u}) + \mathbf{N}(\mathbf{N}^T \mathbf{N})^{-1} \mathbf{F}(\mathbf{F}^T \mathbf{F})^{-1} \mathbf{z}_1(t, \mathbf{u})\right) - \frac{u_o(t)}{V}\mathbf{z}_3(t, \mathbf{u}), \quad (20)$$

with  $\mathbf{z}_3(t_0, \mathbf{u}) \in Z_{3,0} \subset \mathbb{R}^{n_r}$ , where

$$Z_{3,0} \equiv [\mathbf{z}_{3,0}^L, \mathbf{z}_{3,0}^U] = \mathbf{S}^+(\mathbf{I}_{n_x} - \mathbf{W}\mathbf{M}^+ \mathbf{N}^T) [\mathbf{x}_0^L, \mathbf{x}_0^U]. \quad (21)$$

Since (20) is a function of a possibly nonlinear rate function  $\mathbf{r}$ , in general, the IVP (20) does not lend itself to any

analytical solution. As discussed in [2], a tighter enclosure for  $\mathbf{z}_3$  is obtained by implementing Theorem 1 with (4) as compared to (3). Thus if  $G_{z_3}$  denotes an a priori enclosure for the reachable set of  $\mathbf{z}_3$ , then the objective is to design  $G_{z_3}$ . Formally, let  $G_{z_3}$  be such that  $\mathbf{z}_3(t, \mathbf{u}) \in G_{z_3}$  for each  $(\mathbf{z}_{3,0}, \mathbf{u}) \in Z_{3,0} \times \mathcal{U}$  and for all  $t \in T$ . Now, from Theorem 2, the state  $\mathbf{z}_3$  satisfies the transformation relation

$$\mathbf{z}_3(t, \mathbf{u}) = \mathbf{S}^+(\mathbf{I}_{n_x} - \mathbf{W}\mathbf{M}^+\mathbf{N}^T)\mathbf{x}(t, \mathbf{u}). \quad (22)$$

Let  $X^N \equiv [\mathbf{x}^{N,L}, \mathbf{x}^{N,U}]$  be the natural bound for the system, assumed to be known a priori such that  $\mathbf{x}(t, \mathbf{u}) \in X^N$  for each  $(\mathbf{u}, \mathbf{x}_0) \in \mathcal{U} \times X_0$  and for all  $t \in T$ . Now, evaluating an interval extension of (22) over  $X^N$  yields

$$Y_3^{N_1} = \mathbf{S}^+(\mathbf{I}_{n_x} - \mathbf{W}\mathbf{M}^+\mathbf{N}^T)X^N, \quad (23)$$

where  $Y_3^{N_1} \equiv [\mathbf{y}_3^{N_1,L}, \mathbf{y}_3^{N_1,U}]$  is an interval bound for  $\mathbf{z}_3$ , such that  $\mathbf{z}_3(t, \mathbf{u}) \in Y_3^{N_1}$  for all  $(\mathbf{u}, \mathbf{z}_{3,0}) \in \mathcal{U} \times Z_{3,0}$  and for all  $t \in T$ .  $Y_3^{N_1}$  is the natural bound on  $\mathbf{z}_3$  since its construction is based on the use of natural bound information for  $\mathbf{x}$ . Fortunately, it is possible to reduce conservatism, and tighten  $Y_3^{N_1}$  in a post-processing step at an additional computational cost. This is discussed next.

From Theorem 2, observe that in addition to (22),  $\mathbf{z}_3$  also simultaneously satisfies the inverse transformation

$$\begin{aligned} \mathbf{x}(t, \mathbf{u}) &= \mathbf{S}\mathbf{z}_3(t, \mathbf{u}) + \mathbf{W}\mathbf{z}_2(t, \mathbf{u}) \\ &\quad + \mathbf{N}(\mathbf{N}^T\mathbf{N})^{-1}\mathbf{F}(\mathbf{F}^T\mathbf{F})^{-1}\mathbf{z}_1(t, \mathbf{u}). \end{aligned} \quad (24)$$

Given (24), and sets  $Y_3^{N_1}$ ,  $X^N$ ,  $[\mathbf{z}_1]$  and  $[\mathbf{z}_2]$ , the natural bound on  $\mathbf{z}_3$  can be refined by solving the following linear programs

$$\begin{aligned} z_{3,i}^{N,L}(t) &:= \inf_{\mathbf{q}, \mathbf{n}, \mathbf{m}_1, \mathbf{m}_2} q_i \\ \text{s.t. } \mathbf{S}\mathbf{q} &= \mathbf{n} - \mathbf{W}\mathbf{m}_2 - \mathbf{N}(\mathbf{N}^T\mathbf{N})^{-1}\mathbf{F}(\mathbf{F}^T\mathbf{F})^{-1}\mathbf{m}_1, \\ \mathbf{y}_3^{N_1,L} &\leq \mathbf{q} \leq \mathbf{y}_3^{N_1,U}, \\ \mathbf{x}^{N,L} &\leq \mathbf{n} \leq \mathbf{x}^{N,U}, \\ \mathbf{z}_1^L(t) &\leq \mathbf{m}_1 \leq \mathbf{z}_1^U(t), \\ \mathbf{z}_2^L(t) &\leq \mathbf{m}_2 \leq \mathbf{z}_2^U(t), \end{aligned} \quad (25)$$

$$\begin{aligned} z_{3,i}^{N,U}(t) &:= \sup_{\mathbf{q}, \mathbf{n}, \mathbf{m}_1, \mathbf{m}_2} q_i \\ \text{s.t. } \mathbf{S}\mathbf{q} &= \mathbf{n} - \mathbf{W}\mathbf{m}_2 - \mathbf{N}(\mathbf{N}^T\mathbf{N})^{-1}\mathbf{F}(\mathbf{F}^T\mathbf{F})^{-1}\mathbf{m}_1, \\ \mathbf{y}_3^{N_1,L} &\leq \mathbf{q} \leq \mathbf{y}_3^{N_1,U}, \\ \mathbf{x}^{N,L} &\leq \mathbf{n} \leq \mathbf{x}^{N,U}, \\ \mathbf{z}_1^L(t) &\leq \mathbf{m}_1 \leq \mathbf{z}_1^U(t), \\ \mathbf{z}_2^L(t) &\leq \mathbf{m}_2 \leq \mathbf{z}_2^U(t), \end{aligned} \quad (26)$$

for each  $i = 1, \dots, n_r$ . If  $Z_3^N(t) \equiv [\mathbf{z}_3^{N,L}(t), \mathbf{z}_3^{N,U}(t)]$ , then  $Z_3^N$  is the refined natural bound for  $\mathbf{z}_3$ .

The refinement step is optional, and can be invoked at the discretion of the user. With the natural bounds,  $Z_3^N$ ,

the a priori set  $G_{z_3}$  for  $\mathbf{z}_3$  can be defined as follows

$$G_{z_3}(t) \equiv \left\{ \mathbf{y} \in \mathbb{R}^{n_r} : \begin{bmatrix} \mathbf{I}_{n_r} \\ -\mathbf{I}_{n_r} \end{bmatrix} \mathbf{y} \leq \begin{bmatrix} \mathbf{z}_3^{N,U}(t) \\ -\mathbf{z}_3^{N,L}(t) \end{bmatrix} \right\}. \quad (27)$$

In (27), the enclosure set  $G_{z_3}$  is defined explicitly in terms of the natural bounds on  $\mathbf{z}_3$ ; however, other information can also be readily used to describe the set  $G_{z_3}$ . For example, recall that  $Z_3^N$  in (25)-(26) is constructed by first starting with the transformation (22) and then using the inverse transformation (24) in the post-refinement step. Note that if this order of use is switched, it leads to refined natural bounds on  $\mathbf{S}\mathbf{z}_3$  – a linear combination of  $\mathbf{z}_3$ , as shown next.

Writing inverse transformation (24) in terms of  $\mathbf{z}_3$

$$\begin{aligned} \mathbf{S}\mathbf{z}_3(t, \mathbf{u}) &= \mathbf{x}(t, \mathbf{u}) - \mathbf{W}\mathbf{z}_2(t, \mathbf{u}) \\ &\quad - \mathbf{N}(\mathbf{N}^T\mathbf{N})^{-1}\mathbf{F}(\mathbf{F}^T\mathbf{F})^{-1}\mathbf{z}_1(t, \mathbf{u}). \end{aligned} \quad (28)$$

The interval extension of (28) over  $X^N$ ,  $[\mathbf{z}_1]$  and  $[\mathbf{z}_2]$  gives

$$Y_3^{N_2} = X^N - \mathbf{W}[\mathbf{z}_2] - \mathbf{N}(\mathbf{N}^T\mathbf{N})^{-1}\mathbf{F}(\mathbf{F}^T\mathbf{F})^{-1}[\mathbf{z}_1], \quad (29)$$

where  $Y_3^{N_2} \equiv [\mathbf{y}_3^{N_2,L}, \mathbf{y}_3^{N_2,U}]$  is the natural bound on  $\mathbf{S}\mathbf{z}_3$ , such that  $\mathbf{S}\mathbf{z}_3(t, \mathbf{u}) \in Y_3^{N_2}(t)$  for all  $(\mathbf{u}, \mathbf{z}_{3,0}) \in \mathcal{U} \times Z_{3,0}$  and for all  $t \in T$ .

As discussed for  $Y_3^{N_1}$ , it is also possible to refine  $Y_3^{N_2}$  in (29) in a post-processing step using transformation (22). First, observe that pre-multiplying (22) with  $\mathbf{S}$  gives

$$\mathbf{S}\mathbf{z}_3(t, \mathbf{u}) = \mathbf{S}\mathbf{S}^+(\mathbf{I}_{n_x} - \mathbf{W}\mathbf{M}^+\mathbf{N}^T)\mathbf{x}(t, \mathbf{u}). \quad (30)$$

Given (30), and sets  $Y_3^{N_2}$ , and  $X^N$ , the natural bound on  $\mathbf{S}\mathbf{z}_3$  can be refined by solving the following linear programs

$$\begin{aligned} b_{3,i}^{N,L}(t) &:= \inf_{\mathbf{q}, \mathbf{n}} q_i \\ \text{s.t. } \mathbf{q} &= \mathbf{S}\mathbf{S}^+(\mathbf{I}_{n_x} - \mathbf{W}\mathbf{M}^+\mathbf{N}^T)\mathbf{n}, \\ \mathbf{y}_3^{N_2,L}(t) &\leq \mathbf{q} \leq \mathbf{y}_3^{N_2,U}(t), \\ \mathbf{x}^{N,L} &\leq \mathbf{n} \leq \mathbf{x}^{N,U}, \end{aligned} \quad (31)$$

$$\begin{aligned} b_{3,i}^{N,U}(t) &:= \sup_{\mathbf{q}, \mathbf{n}} q_i \\ \text{s.t. } \mathbf{q} &= \mathbf{S}\mathbf{S}^+(\mathbf{I}_{n_x} - \mathbf{W}\mathbf{M}^+\mathbf{N}^T)\mathbf{n}, \\ \mathbf{y}_3^{N_2,L}(t) &\leq \mathbf{q} \leq \mathbf{y}_3^{N_2,U}(t), \\ \mathbf{x}^{N,L} &\leq \mathbf{n} \leq \mathbf{x}^{N,U}, \end{aligned} \quad (32)$$

for each  $i = 1, \dots, n_r$ . Now, if  $B_3^N(t) \equiv [\mathbf{b}_3^{N,L}(t), \mathbf{b}_3^{N,U}(t)]$ , then  $B_3^N$  is the refined natural bound for  $\mathbf{S}\mathbf{z}_3$ . Again, the post-refinement step is optional, and can be invoked when required. With  $B_3^N$  computed,  $G_{z_3}$  can be defined as

$$G_{z_3}(t) = \left\{ \mathbf{y} \in \mathbb{R}^{n_r} : \begin{bmatrix} \mathbf{S} \\ -\mathbf{S} \end{bmatrix} \mathbf{y} \leq \begin{bmatrix} \mathbf{b}_3^{N,U}(t) \\ -\mathbf{b}_3^{N,L}(t) \end{bmatrix} \right\}. \quad (33)$$



Since a unique strategy to design  $G_{z_3}$  may not exist for a given system, as for  $G_x$ , we construct  $G_{z_3}$  by combining (27) and (33) to get

$$G_{z_3}(t) = \left\{ \mathbf{y} \in \mathbb{R}^{n_r} : \begin{bmatrix} \mathbf{I}_{n_r} \\ -\mathbf{I}_{n_r} \\ \mathbf{S} \\ -\mathbf{S} \end{bmatrix} \mathbf{y} \leq \begin{bmatrix} \mathbf{z}_3^{N,U}(t) \\ -\mathbf{z}_3^{N,L}(t) \\ \mathbf{b}_3^{N,U}(t) \\ -\mathbf{b}_3^{N,L}(t) \end{bmatrix} \right\}. \quad (34)$$

In general, due to additional inequalities included, (34) is at least as tight as (27) or (33). Now, with  $G_{z_3}$  defined in (34), enclosures for  $\mathbf{z}_3$  can be computed using Theorem 1 with (4). Here, note that since  $G_{z_3}$  is a polyhedral set defined by the intersection of  $2(n_r + n_x)$  half-spaces, the interval-tightening operation over set  $G_{z_3}$  in (4) can be constructed using the algorithm discussed in Definition 4 in [17].

Let  $[\mathbf{z}_3] \equiv [\mathbf{z}_3^L, \mathbf{z}_3^U]$  denote an enclosure for  $\mathbf{z}_3$ , computed using the procedure discussed in this section, then

$$\mathbf{z}_3^L(t) \leq \mathbf{z}_3(t, \mathbf{u}) \leq \mathbf{z}_3^U(t), \quad (35)$$

holds for each  $(\mathbf{u}, \mathbf{z}_{3,0}) \in \mathcal{U} \times Z_{3,0}$  and for all  $t \in T$ .

#### 4.2.4. Summary of bounds on $\mathbf{z}$

Let  $[\mathbf{z}] \equiv [\mathbf{z}^L, \mathbf{z}^U]$  denote an enclosure for the reachable set of the CSTR reaction system in the transformed state space as described by the IVP in Theorem 2. Then from (10), (17) and (35), we have  $[\mathbf{z}] = [\mathbf{z}_1] \times [\mathbf{z}_2] \times [\mathbf{z}_3]$  such that

$$\mathbf{z}^L(t) \equiv \begin{bmatrix} \mathbf{z}_1^L(t) \\ \mathbf{z}_2^L(t) \\ \mathbf{z}_3^L(t) \end{bmatrix} \leq \mathbf{z}(t, \mathbf{u}) \leq \begin{bmatrix} \mathbf{z}_1^U(t) \\ \mathbf{z}_2^U(t) \\ \mathbf{z}_3^U(t) \end{bmatrix} \equiv \mathbf{z}^U(t), \quad (36)$$

holds for each  $(\mathbf{u}, \mathbf{z}_0) \in \mathcal{U} \times Z_0$  and for all  $t \in T$ , where the set of initial conditions is defined as  $Z_0 = Z_{1,0} \times Z_{2,0} \times Z_{3,0}$ .

Observe that, unlike  $[\mathbf{z}_1]$  and  $[\mathbf{z}_2]$ , enclosure  $[\mathbf{z}_3]$  overestimates the reachable set  $\mathbf{z}_3(t, \mathcal{U})$ . The degree of conservatism in  $[\mathbf{z}_3]$  depends on the efficiency of interval methods in implementing Theorem 1 for the IVP (20). Fortunately, the sparse representation of the IVP (20), combined with a reasonable a priori enclosure in (34) help reduce overestimation due to the dependency problem and wrapping effect discussed in Section 3.1. Further, notice that the sparse representation in Theorem 2 limits the overestimation in  $[\mathbf{z}]$  in (36) only to  $n_r$  out of  $n_x$  states in  $\mathbf{z}$ .

#### 4.3. Step 3: Reconstruction

It is important to highlight that while Section 4.2 provides an efficient approach to compute enclosures of CSTR reaction systems in the transformed state space, the objective is to compute bounds in the original state space. In this section, we discuss the procedure for reconstructing enclosures for  $\mathbf{x}$  using the enclosures for  $\mathbf{z}$  computed in Section 4.2. This constitutes Step 3 of the indirect-bounding

method proposed in Section 4. In the remainder of this section, we make no further reference to the procedure for computing  $[\mathbf{z}]$ , and instead assume  $[\mathbf{z}]$  is available at our disposal from Section 4.2.

The simplest approach to reconstruct  $[\mathbf{x}]$  from  $[\mathbf{z}]$  is to use the inverse transformation relation in Theorem 2. Evaluating an interval extension of the inverse transformation relation in (7b) over  $[\mathbf{z}]$  yields

$$[\mathbf{x}] = \mathbf{S}[\mathbf{z}_3] + \mathbf{W}[\mathbf{z}_2] + \mathbf{N}(\mathbf{N}^T \mathbf{N})^{-1} \mathbf{F}(\mathbf{F}^T \mathbf{F})^{-1} [\mathbf{z}_1], \quad (37)$$

where  $[\mathbf{x}] \equiv [\mathbf{x}^L, \mathbf{x}^U]$  is the required state bound on  $\mathbf{x}$ , and  $[\mathbf{z}_1]$ ,  $[\mathbf{z}_2]$  and  $[\mathbf{z}_3]$  are the state bounds for  $\mathbf{z}_1$ ,  $\mathbf{z}_2$  and  $\mathbf{z}_3$ , respectively. Observe that although (37) is a valid enclosure for  $\mathbf{x}$ , it is conservative. This is because the interval extension in (37) evaluates to the interval hull of the image set. In addition, in (37), the relationship between  $\mathbf{z}$  and  $\mathbf{x}$  is not explicitly accounted for, i.e., the variables  $\mathbf{z}_1$ ,  $\mathbf{z}_2$ , and  $\mathbf{z}_3$  are allowed to assume arbitrarily values in  $[\mathbf{z}_1]$ ,  $[\mathbf{z}_2]$  and  $[\mathbf{z}_3]$  independent of  $\mathbf{x}$ , such that (37) conservatively accounts for every triplet  $(\mathbf{z}_1, \mathbf{z}_2, \mathbf{z}_3) \in [\mathbf{z}_1] \times [\mathbf{z}_2] \times [\mathbf{z}_3]$ .

**Remark 1.** The conservatism in (37) due to the dependency problem is localized only to the time instant at which  $[\mathbf{x}]$  is computed. There is no conservatism build-up (see Section 3.1) in  $[\mathbf{x}]$  over time as interval extension computed at any two time instants in (37) are independent of one another, with no temporal feedback of intervals.

To improve enclosure computation in (37), we need to enforce the underlying relationship between  $\mathbf{z}$  and  $\mathbf{x}$ . This is explored in the next section.

##### 4.3.1. Bounds Tightening

To improve the bound computation in (37), we apply the transformation in (7a) to enforce the relationship between  $\mathbf{x}$  and  $\mathbf{z}$ . According to Theorem 2, given  $\mathbf{z}(t, \mathbf{u})$ , the state  $\mathbf{x}(t, \mathbf{u})$  can only assume a value that satisfies

$$\begin{bmatrix} \mathbf{F}^T \mathbf{N}^T \\ \mathbf{M}^+ \mathbf{N}^T \\ \mathbf{S}^+ (\mathbf{I}_{n_x} - \mathbf{W} \mathbf{M}^+ \mathbf{N}^T) \end{bmatrix} \mathbf{x}(t, \mathbf{u}) = \begin{bmatrix} \mathbf{z}_1(t, \mathbf{u}) \\ \mathbf{z}_2(t, \mathbf{u}) \\ \mathbf{z}_3(t, \mathbf{u}) \end{bmatrix}. \quad (38)$$

Now, observe that each of the variables  $\mathbf{z}_1 \in [\mathbf{z}_1]$ ,  $\mathbf{z}_2 \in [\mathbf{z}_2]$  and  $\mathbf{z}_3 \in [\mathbf{z}_3]$  independently constraint  $\mathbf{x}$  to specific sets. For example, an interval extension of the first equality in (38) over  $[\mathbf{z}_1]$  constraints  $\mathbf{x}$ , such that

$$\mathbf{z}_1^L(t) \leq \mathbf{F}^T \mathbf{N}^T \mathbf{x}(t, \mathbf{u}) \leq \mathbf{z}_1^U(t), \quad (39)$$

holds for each  $(\mathbf{u}, \mathbf{x}_0) \in \mathcal{U} \times X_0$  and for all  $t \in T$ . In fact, observe that (39) hold for all  $\mathbf{z}_2 \in [\mathbf{z}_2]$  and  $\mathbf{z}_3 \in [\mathbf{z}_3]$ . Similarly, evaluating interval extensions for every equality in (38), and putting them together gives

$$\begin{bmatrix} \mathbf{z}_1^L(t) \\ \mathbf{z}_2^L(t) \\ \mathbf{z}_3^L(t) \end{bmatrix} \leq \mathbf{A}_1 \mathbf{x}(t, \mathbf{u}) \leq \begin{bmatrix} \mathbf{z}_1^U(t) \\ \mathbf{z}_2^U(t) \\ \mathbf{z}_3^U(t) \end{bmatrix}, \quad (40)$$

which holds for each  $(\mathbf{u}, \mathbf{x}_0) \in \mathcal{U} \times X_0$  and for all  $t \in T$ . In (40),  $\mathbf{A}_1 \in \mathbb{R}^{n_x \times n_x}$  is defined as

$$\mathbf{A}_1 = \begin{bmatrix} \mathbf{F}^T \mathbf{N}^T \\ \mathbf{M}^+ \mathbf{N}^T \\ \mathbf{S}^+ (\mathbf{I}_{n_x} - \mathbf{W} \mathbf{M}^+ \mathbf{N}^T) \end{bmatrix}.$$

As compared to (37), the relations between  $\mathbf{x}$  and  $\mathbf{z}_1, \mathbf{z}_2, \mathbf{z}_3$  are explicit in (40). Furthermore, from the natural bounds  $X^N$  on  $\mathbf{x}$ , assumed to be available a priori (see Section 4.2.3), we also know that the inequality

$$\mathbf{x}^{N,L} \leq \mathbf{x}(t, \mathbf{u}) \leq \mathbf{x}^{N,U}, \quad (41)$$

holds for each  $(\mathbf{u}, \mathbf{x}_0) \in \mathcal{U} \times X_0$  and for all  $t \in T$ . Equations (40) and (41) can be compactly represented as follows

$$H_x(t) \equiv \{\mathbf{y} \in \mathbb{R}^{n_x} : \mathbf{A} \mathbf{y} \leq \mathbf{m}(t)\}, \quad (42)$$

for all  $t \in T$ , where  $\mathbf{A} \in \mathbb{R}^{4n_x \times n_x}$  and  $\mathbf{m}(t) \in \mathbb{R}^{4n_x}$  are

$$\mathbf{A} = \begin{bmatrix} \mathbf{I}_{n_x} \\ -\mathbf{I}_{n_x} \\ \mathbf{F}^T \mathbf{N}^T \\ -\mathbf{F}^T \mathbf{N}^T \\ \mathbf{M}^+ \mathbf{N}^T \\ -\mathbf{M}^+ \mathbf{N}^T \\ \mathbf{S}^+ (\mathbf{I}_{n_x} - \mathbf{W} \mathbf{M}^+ \mathbf{N}^T) \\ -\mathbf{S}^+ (\mathbf{I}_{n_x} - \mathbf{W} \mathbf{M}^+ \mathbf{N}^T) \end{bmatrix}; \quad \mathbf{m}(t) = \begin{bmatrix} \mathbf{x}^{N,U} \\ -\mathbf{x}^{N,L} \\ \mathbf{z}_1^U(t) \\ -\mathbf{z}_1^L(t) \\ \mathbf{z}_2^U(t) \\ -\mathbf{z}_2^L(t) \\ \mathbf{z}_3^U(t) \\ -\mathbf{z}_3^L(t) \end{bmatrix}.$$

In (42),  $H_x(t)$  is a polyhedral set defined by the intersection of  $4n_x$  half-spaces. It is instructive to highlight that  $H_x(t)$  by itself also describes a valid enclosure for  $\mathbf{x}(t, \mathcal{U})$  for all  $t \in T$ ; however,  $H_x(t)$  is a polyhedral enclosure, and not an interval enclosure sought in this paper. Nevertheless, it is possible to leverage the polyhedral enclosure information in (42) to tighten the interval bounds in (37). This is done through the interval-tightening operation  $\mathcal{P}_{H_x}$  used in Section 3 over  $H_x$ . The interval-tightening operation is discussed next.

**Definition 1.** (Interval-tightening, [17]) Let  $D_{\mathcal{P}} \subset \mathbb{IR}^{n_x}$  be defined such that  $\{Y \in \mathbb{IR}^{n_x} : Y \cap H_x \neq \emptyset\} \subset D_{\mathcal{P}}$  and let  $\mathcal{P}_{H_x} : D_{\mathcal{P}} \rightarrow \mathbb{IR}^{n_x}$  be a Lipschitz mapping satisfying

1.  $\mathcal{P}_{H_x}(Y) \subset Y$  for all  $Y \in D_{\mathcal{P}}$  with  $Y \cap H_x \neq \emptyset$ ,
2. For  $Y \in D_{\mathcal{P}}$ , if  $\mathbf{y} \in Y$  and  $\mathbf{y} \notin \mathcal{P}_{H_x}(Y)$ , then  $\mathbf{y} \notin H_x$ .

In Definition 1, the Lipschitz mapping,  $\mathcal{P}_{H_x}$ , takes an interval argument,  $Y \in D_{\mathcal{P}}$ , and tightens it by discarding points in the interval which are not in set  $H_x$ . Thus  $\mathcal{P}_{H_x}([\mathbf{x}])$  is a refinement of  $[\mathbf{x}]$  computed in (37). For a polyhedral  $H_x$ , the mapping  $\mathcal{P}_{H_x}$  can be constructed using Definition 4 in [17]. The main steps are repeated in Algorithm 1 for the sake of completeness. Algorithm 1 takes an interval enclosure available from (37) and tightens it by excluding points that are not in  $H_x$ . The resulting tightened set is also an interval. Figure 2 gives a schematic of the interval-tightening operation defined in Algorithm 1.

---

#### Algorithm 1 Interval-tightening – $\mathcal{P}_{H_x}$

---

**Input:**  $\mathbf{A} \in \mathbb{R}^{4n_x \times n_x}$ ,  $\mathbf{m} \in \mathbb{R}^{4n_x}$ ,  $[\mathbf{x}^L(t), \mathbf{x}^U(t)]$

**Output:**  $\mathcal{P}_{H_x}([\mathbf{x}^L(t), \mathbf{x}^U(t)])$

```

1:  $[\mathbf{v}, \mathbf{w}] \leftarrow [\mathbf{x}^L(t), \mathbf{x}^U(t)]$ .
2: for  $j = 1$  to  $n_x$  do
3:   for  $i = 1$  to  $4n_x$  do
4:     if  $a_{i,j} \neq 0$  then
5:        $\kappa \leftarrow \text{med}\{1/a_{i,j} \sum_{k \neq j} \max(-a_{i,k} v_k - a_{i,k} w_k) + b_{i,j}, v_j, w_j\}$ .
6:       if  $a_{i,j} > 0$  then
7:          $w_j \leftarrow \kappa$ .
8:       end if
9:       if  $a_{i,j} < 0$  then
10:         $v_j \leftarrow \kappa$ .
11:      end if
12:    end if
13:  end for
14: end for
15: return  $\mathcal{P}_{H_x}([\mathbf{x}^L(t), \mathbf{x}^U(t)]) \leftarrow [\mathbf{v}, \mathbf{w}]$ 
```

---

**Remark 2.** The interval-tightening operation,  $\mathcal{P}_{H_x}$ , defined in Algorithm 1 is applied point-wise in time to tighten  $[\mathbf{x}]$  in a post-processing step. Since the operation is non-recursive, it can be automated on a parallel computer, or appealed to only at those times where  $[\mathbf{x}]$  is sought.

Finally, Sections 4.1 – 4.3 describe the indirect-bounding method outlined in Section 4 for computing interval enclosures for the reachable set of a CSTR reaction system described in (1). The algorithm to implement the indirect-bounding method is discussed in Algorithm 2 and its efficacy demonstrated in Section 8.

## 5. Comparing Indirect and Direct Methods

In this paper, and in [2], we propose two bounding methods – indirect and direct methods – for computing interval enclosures for the reachable set of a CSTR reaction system. In this section, we qualitatively compare the direct and indirect methods based on their design, and comment on their expected performance and computational cost.

In terms of design, both direct and indirect methods apply Theorem 2 to compute enclosures for the CSTR reaction system; however, there is a significant difference in the way Theorem 2 is applied by the two methods. While the indirect-bounding method applies Theorem 2 to map the system into the transformed state space, the direct-bounding method applies Theorem 2 to provide an efficient a priori enclosure for the system in the original state space. In other words, the indirect method applies Theorem 1 to yield enclosures in the transformed space, the direct method applies Theorem 1 to bound the system in the original space. This constitutes the basic difference between the indirect and direct methods in terms of their design.

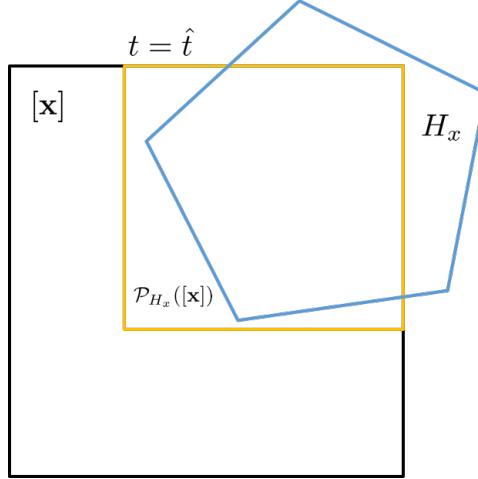


Figure 2: An illustration of the bound tightening operation  $\mathcal{P}_{H_x}$ . The interval-tightening operator  $\mathcal{P}_{H_x}$  takes an interval  $[\mathbf{x}]$  and returns a refined interval  $\mathcal{P}_{H_x}([\mathbf{x}])$ , by discarding points in  $[\mathbf{x}]$ , not contained in set  $H_x$ . Note that the bound tightening step produces an interval enclosure of the intersection of  $H_x$  and  $[\mathbf{x}]$ , but not necessarily the interval hull of the intersection.

A rigorous comparison of the performance of the direct and indirect bounding methods is beyond the scope of the current work; however, qualitatively, it appears that the indirect-bounding method yields tighter enclosures in general than the direct-bounding method. This is because of the effectiveness of bounding CSTR reaction systems in the transformed state space. Note that in the transformed state space,  $n_x - n_r$  states in  $\mathbf{z}$  can be exactly enclosed using the procedure outlined in Sections 4.2.1 and 4.2.2, while the remaining  $n_r$  states can be effectively enclosed as described in Section 4.2.3. Further, in the indirect-bounding method, the conservatism does not build-up over time while reconstructing  $[\mathbf{x}]$  from  $[\mathbf{z}]$  (see Remark 1); whereas, for the direct-bounding method, although an a priori enclosure  $G_x$  keeps conservatism in  $[\mathbf{x}]$  in check, it may still grow over time depending on the complexity of (1) and the quality of  $G_x$  (see Section 3.1). Note that the comparison of performance here is strictly qualitative, and cannot be generalized for all CSTR reaction systems or for all the states.

Finally, the indirect-bounding method is cheaper to implement. The main computational cost associated with the indirect method is the enclosure computation step for  $\mathbf{z}_3$ . As discussed in Section 4.2, unlike for the states  $\mathbf{z}_1$  and  $\mathbf{z}_2$  – for which closed-form analytical bounding solutions exist – computing an efficient enclosure for  $\mathbf{z}_3$  requires the application of Theorem 1 with (4). This in turn requires solving  $2(n_r + n_x)$  linear programs to construct  $G_{z_3}$  in (34) at each integration time. Now, unlike the indirect-bounding method, where Theorem 1 is implemented only on a  $n_r$ -dimensional IVP in (20), the direct-bounding method implements Theorem 1 on a  $n_x$ -dimensional IVP in (1). This adds to the computational cost of the direct method as  $n_x > n_r$  (see Hypothesis 3 in Theorem 2). Further, generating  $G_x$  for a CSTR reaction system in the original state space requires solving  $6n_x$  linear programs at each

integration time [2], which also substantially adds to the computational cost of implementing the direct-bounding method.

In summary, compared to the direct-bounding method, the indirect method yields tighter enclosures for the reachable sets of CSTR reaction systems in (1), and is also computationally cheaper to implement. This claim is only qualitative, as deducing any generalized conclusions on the performance of the indirect and direct methods is beyond the scope of this paper. Nevertheless, we validate the claims made in this section in Section 8 on simulation examples.

## 6. Final Algorithm

In this section, we summarize the developments of Section 4, and present an algorithm for computing interval enclosures for the reachable set of a CSTR reaction system using the indirect-bounding method. A flowchart for the indirect-bounding method is given in Figure 3, and the computational steps involved summarized in Algorithm 2. From Figure 3, given a CSTR reaction system in (1) and corresponding interval sets  $X_0, U, T, X^N$ , as discussed in Section 4, the indirect method is decomposed into three steps. The first step in Figure 3 (or Step 1 in Algorithm 2) applies Theorem 2 to map the CSTR reaction system into the transformed state space, where the dynamics are described by  $\mathbf{z}$ . In the second step (or Steps 2 through 7 in Algorithm 2), by exploiting the correlation between  $\mathbf{z}$ , we compute  $[\mathbf{z}]$  using analytical methods for states  $\mathbf{z}_1$ , and  $\mathbf{z}_2$ , and Theorem 1 for state  $\mathbf{z}_3$ . In the final step (or Steps 8 and 9 in Algorithm 2), an enclosure  $[\mathbf{x}]$ , is reconstructed using  $[\mathbf{z}]$ . The interval-tightening operation is used on  $[\mathbf{x}]$  as a post-refinement step to tighten  $[\mathbf{x}]$  based on set  $H_x$ .

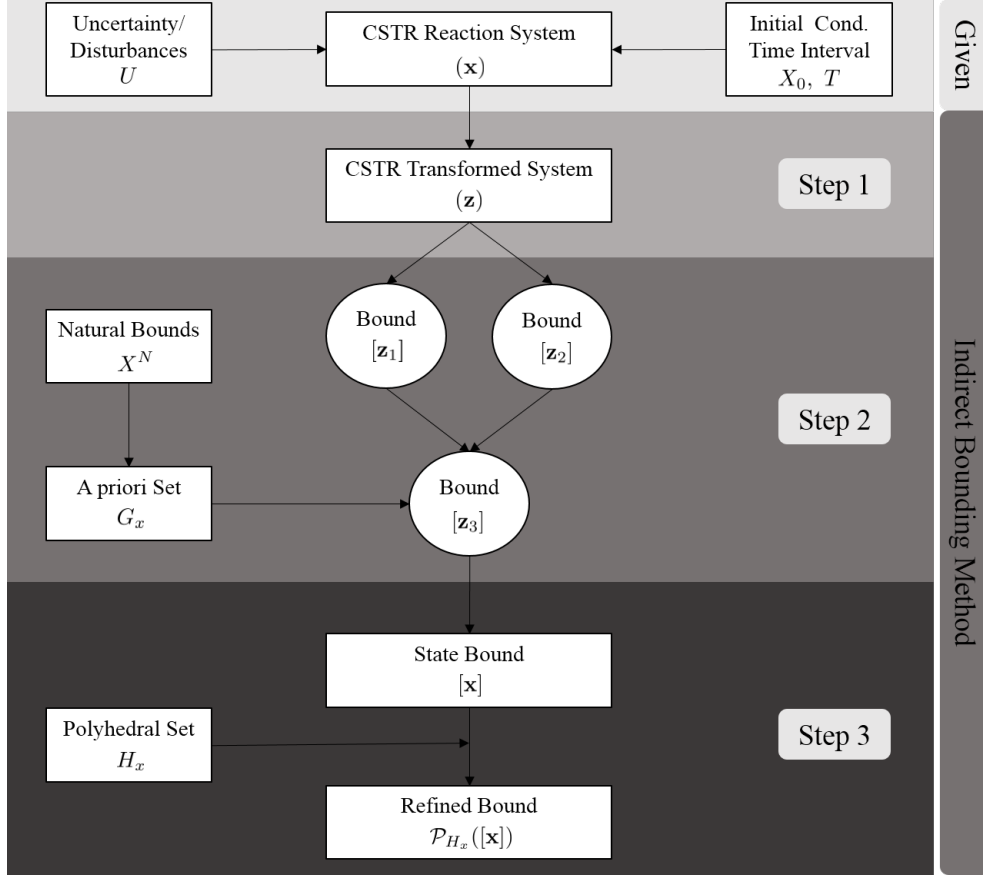


Figure 3: A flowchart for the indirect-bounding method for computing interval enclosure for the reachable set of a CSTR reaction system described by (1).

### Algorithm 2 Indirect Bounding Method

**Input:** Model (1) satisfying Hypotheses (1) through (4) in Theorem 2, and sets  $U$ ,  $X_0$ , and  $X^N$

**Output:** State bounds  $[\mathbf{x}]$

- 1: Apply Theorem 2 to transform  $\mathbf{x}$  to  $\mathbf{z}$ .
- 2: Compute  $Z_{1,0}$  using (9). Calculate  $[\mathbf{z}_1]$  using (12).
- 3: Compute  $Z_{2,0}$  using (14). If  $n_p = 1$ , calculate  $[\mathbf{z}_2]$  using (19) or (16) otherwise.
- 4: Compute  $Y_3^{N_1}$  using (23). Use (25)-(26) to refine  $Y_3^{N_1}$  (optional) or set  $Z_3^N = Y_3^{N_1}$ .
- 5: Compute  $Y_3^{N_2}$  using (29). Use (31)-(32) to refine  $Y_3^{N_2}$  (optional) or set  $B_3^N = Y_3^{N_2}$ .
- 6: Compute  $G_{z_3}$  using (34).
- 7: Compute  $Z_{3,0}$  using (21). Calculate  $[\mathbf{z}_3]$  using Theorem 1 with (4) on the IVP (20).
- 8: Compute  $[\mathbf{x}]$  using (37).
- 9: Compute  $H_x$  in (42). Use Algorithm 1 to compute  $\mathcal{P}_{H_x}([\mathbf{x}])$ .
- 10: **return**  $[\mathbf{x}] \leftarrow \mathcal{P}_{H_x}([\mathbf{x}])$

## 7. Implementation

Implementing Algorithm 2 manually on a computer is a tedious and an error-prone task. Fortunately, it is possible to

automate the steps in Algorithm 2 in MATLAB. The examples in Section 8 are coded in a custom MATLAB code; however, other computing platforms, such as C++ and FORTRAN can also be readily used to implement Algorithm 2.

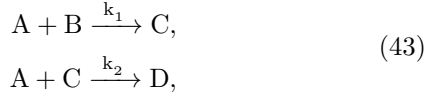
The transformation of the CSTR reaction system, as required by Step 1 in Algorithm 2, is calculated from (1) using matrices  $\mathbf{N}$ ,  $\mathbf{F}$ ,  $\mathbf{S}^+$  and  $\mathbf{M}^+$  (see Theorem 2). In MATLAB, the required matrices can be automatically computed using routines `null` and `pinv`. The main challenge is to evaluate natural interval extensions in Steps 2 through 5 in Algorithm 2. The interval extensions can be reliably computed using a commercial MATLAB toolbox INTLAB or a publicly available C++ library MC++. For a detailed description of INTLAB and MC++, see [23, 24]. The optional natural bound refinement in Steps 4 and 5 in Algorithm 2 are computed in MATLAB using routine `linprog`. The interval extension of the right-hand-side function of the IVP, required for computing  $[\mathbf{z}_3]$  in Step 7 in Algorithm 2 was manually coded, but can be automated using INTLAB or MC++. Finally the numerical integration of IVPs is performed in MATLAB using routine `ode15s`. In C++ numerical integration can be performed using CVODE [25].

Finally, all computations are done in MATLAB R2013b running on a Dell Precision T3500 workstation with a 3.20 GHz Intel Xenon CPU.

## 8. Numerical Examples

We present two examples to demonstrate the efficacy of the indirect-bounding method outlined in Algorithm 2 for computing interval enclosures for the reachable sets of CSTR reaction systems. Example 2 is a 4-species irreversible reaction network adapted from [22], and Example 3 is a 7-species reversible reaction network from [26].

**Example 2.** Consider the chemical reaction network



with forward and reverse rate constants  $k_1$  and  $k_2$ , respectively, in an isothermal CSTR of volume  $V = 20$  liters. For the reaction network (43), we have  $n_r = 2$  and  $n_x = 4$ . Let  $\mathbf{x} = [x_1 \ x_2 \ x_3 \ x_4]^T$  denote the molar concentrations of the species A, B, C, and D, respectively, with the initial concentrations given by  $\mathbf{x}_0 = [0.1 \ 0 \ 0 \ 0]^T$  (M). The evolution of  $\mathbf{x}$  in the CSTR can be described by (1). Assuming (43) follows a second-order mass-action kinetics law with  $k_2 = 20 \text{ M}^{-1}\text{s}^{-1}$ , the stoichiometric matrix  $\mathbf{S}$  and the rate function  $\mathbf{r}$  in (1) are described by

$$\mathbf{S} = \begin{bmatrix} -1 & -1 \\ -1 & 0 \\ 1 & -1 \\ 0 & 1 \end{bmatrix}, \quad \mathbf{r} = \begin{bmatrix} k_1 x_1 x_2 \\ 20 x_1 x_3 \end{bmatrix}.$$

Let the CSTR include a single input and output flow rate denoted by  $u_i$  and  $u_o$ , respectively, such that  $n_p = 1$ . Let the concentrations of the species A and B in the input flow rate be 0.05M, such that the concentration matrix,  $\mathbf{W}$  in (1) is described by

$$\mathbf{W} = \begin{bmatrix} 0.05 \\ 0.05 \\ 0 \\ 0 \end{bmatrix}.$$

It is assumed that  $\mathbf{x}_0$  is accurately measured, such that  $X_0 = [0.1, 0.1] \times [0, 0] \times [0, 0] \times [0, 0]$  is a degenerate interval vector in  $\mathbb{R}^4$ . Let  $\mathbf{u} = [k_1 \ u_i \ u_o]^T$  denote a vector of uncertain variables. Now, suppose that  $k_1$  is only known to within an order of magnitude, and the input flow rate variation is within the same order of magnitude, so that  $\mathbf{u}$  is restricted to lie in the interval  $U \equiv [10, 500] \times [0.9, 1.1] \times [0.9, 1.1] \text{ (M}^{-1}\text{s}^{-1}, \text{liters s}^{-1}, \text{liters s}^{-1}\text{)}$ . Here, the variation in the output flow rate is the same as that for the input flow rate, since for  $n_p = 1$ ,  $u_o = u_i$  (see (2)). Further, it is assumed that variation in  $u_i$  is uncertain, but always constant. Finally, since  $k_1$  is the only uncertain model parameter, we have  $n_k = 1$ .

The network (43) satisfies Hypotheses (1) through (4) in Theorem 2 – this is validated by noting that  $\mathbf{S}$  and  $\mathbf{W}$  are full-column rank and the inequality  $n_x > n_r + n_p$

holds. It is straightforward to show that the Hypothesis (4) holds.

The natural bounds  $X^N = [0, 0.2] \times [0, 0.2] \times [0, 0.2] \times [0, 0.2]$  on  $\mathbf{x}$  are given as input.  $X^N$  is conservatively constructed to account for the external input and output flow rates. Given (43) under Hypotheses (1) through (4) in Theorem 2, and intervals  $U, X_0, X^N$ , an enclosure for  $\mathbf{x}$  over  $T = [0, 2]$  is computed using the indirect-bounding method in Algorithm 2.

Figure 4 illustrates the bounding results (dashed red curves) for the CSTR system in the transformed state space, as obtained from Steps 1 through 7 in Algorithm 2. For comparison, trajectories obtained by simulating the CSTR reaction system in the transformed state space for constant random samples of  $\mathbf{u} = [k_1 \ u_i \ u_o]^T \in U \equiv [10, 500] \times [0.9, 1.1] \times [0.9, 1.1] \text{ (M}^{-1}\text{s}^{-1}, \text{liters s}^{-1}, \text{liters s}^{-1}\text{)}$  are also shown.

From Figures 4(a) and (b), it is clear that the upper and lower bounding solutions for the states  $z_1$  and  $z_2$ , computed from Steps 2 and 3 are exact. In other words, there is no overestimation associated with enclosure computations for states  $z_1$  and  $z_2$  (see Sections 4.2.1 and 4.2.2 for explanation). The enclosure for the reachable set of  $\mathbf{z}_3 = [z_{3,1} \ z_{3,2}]^T$ , as computed from Step 7 in Algorithm 2 is shown in Figures 4(c) and (d). Unlike for the states  $z_1$  and  $z_2$ , the enclosure for  $\mathbf{z}_3$  possibly involves some degree of overestimation. This is because computing enclosures by applying Theorem 1 involves a certain degree of overestimation due to the dependency problem and the wrapping effect, as discussed in Section 3.1. Of course, implementing Theorem 1 with (4) results in small overestimation in Figures 4(c) and (d). This is because (4) is implemented with an efficient a priori enclosure  $G_{z_3}$ , designed in (34).

Figure 5 shows enclosures for the reachable set of the CSTR system in the original state space computed with the indirect-bounding method. In Figure 5, the red curves represent the upper and lower bounding solutions for the concentrations of the species A through D. For comparison purposes, sample trajectories are also shown (black curves). The trajectories are obtained by simulating the IVP (1) for random samples of  $\mathbf{u} = [k_1 \ u_i \ u_o]^T \in U \equiv [10, 500] \times [0.9, 1.1] \times [0.9, 1.1] \text{ (M}^{-1}\text{s}^{-1}, \text{liters s}^{-1}, \text{liters s}^{-1}\text{)}$ . It is clear that the indirect-bounding method not only yields valid enclosures for the reachable sets of the CSTR systems, the enclosures computed therefrom are also tight.

Notice that the enclosure for  $\mathbf{x}$  is not exact, as it includes some overestimation; however, the extent of overestimation is certainly limited due to the use of an interval-tightening procedure in Step 9 in Algorithm 2. This is demonstrated in Figure 6, where bounding results obtained with and without the use of an interval-tightening step are shown. The bounding results obtained with the use of interval-tightening step in Figure 6 are obtained from Step 9 in Algorithm 2; whereas, the bounding results without the use of interval-tightening step are obtained from Step 8. It is clear from Figure 6 that in terms of the lower bounding solution for species A, inclusion of an interval-

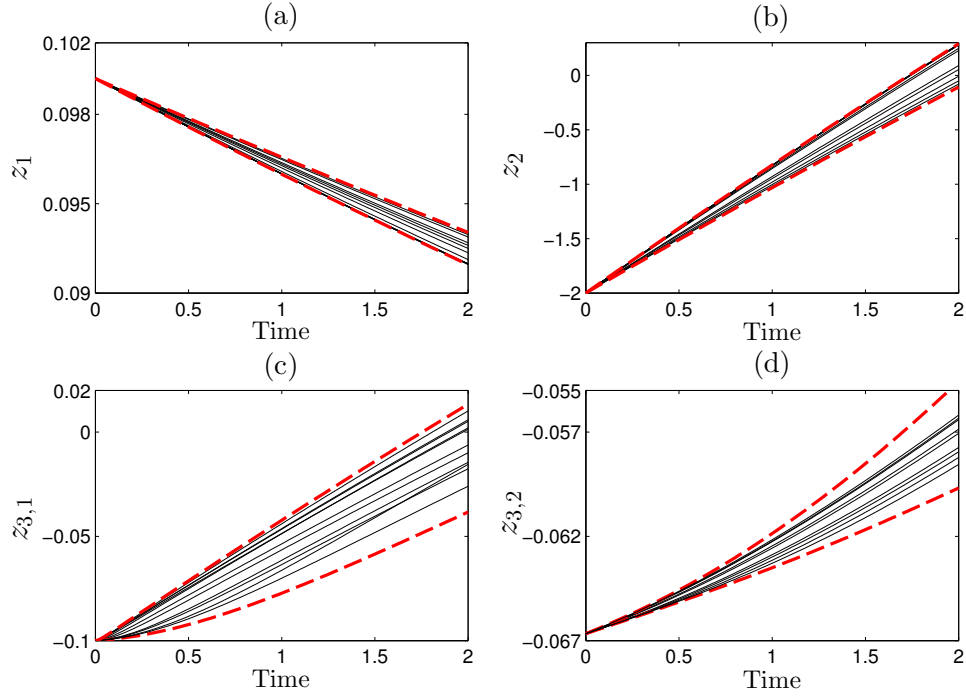


Figure 4: Bounding solutions for species A through D from Example 2 in transformed state space. The bounding solutions are computed using Algorithm 2 with results in sub-figure – (a) computed from Step 2; (b) computed from Step 3; and (c) and (d) from Step 7. In sub-figures (a) through (d), dashed red curves are the upper and lower bounding solutions; and solid curves are concentrations of the species A through D in transformed state space computed by simulating the IVP in Step 1 for constant random samples of  $\mathbf{u} = [k_1 \ u_i \ u_o]^T \in U \equiv [10, 500] \times [0.9, 1.1] \times [0.9, 1.1]$  ( $\text{M}^{-1}\text{s}^{-1}$ ,  $\text{liters s}^{-1}$ ,  $\text{liters s}^{-1}$ ).

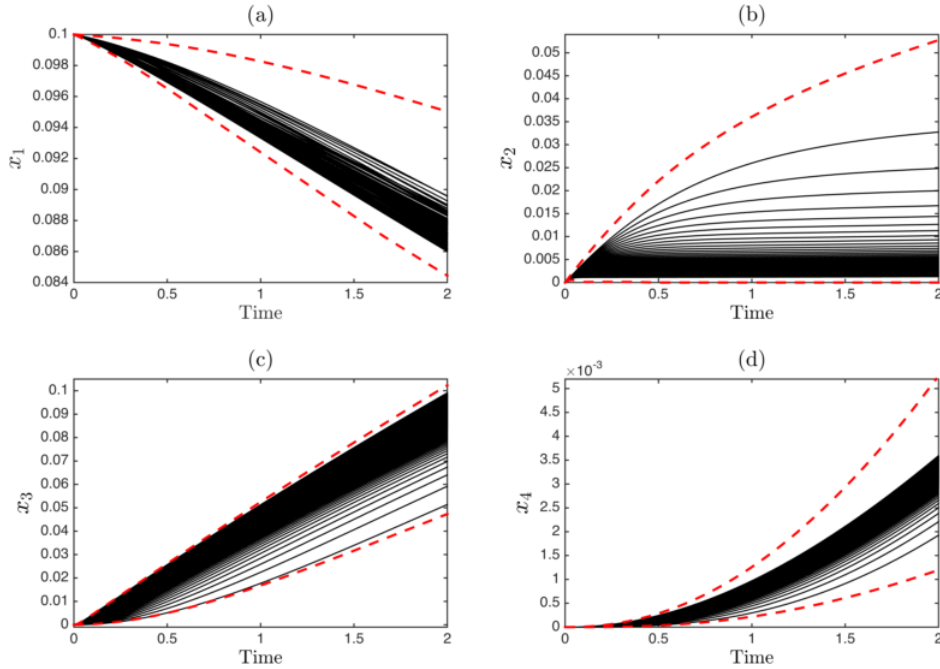


Figure 5: Bounding solutions for species A through D from Example 2 in the original state space. The bounding solutions are computed using Step 10 in Algorithm 2. In sub-figures (a) through (d), dashed red curves are the upper and lower bounding solutions, reconstructed from  $[\mathbf{z}]$  in Figure 4; and solid curves are concentrations of the species A through D in the original state space computed by simulating the CSTR reaction system for constant random samples of  $\mathbf{u} = [k_1 \ u_i \ u_o]^T \in U \equiv [10, 500] \times [0.9, 1.1] \times [0.9, 1.1]$  ( $\text{M}^{-1}\text{s}^{-1}$ ,  $\text{liters s}^{-1}$ ,  $\text{liters s}^{-1}$ ).

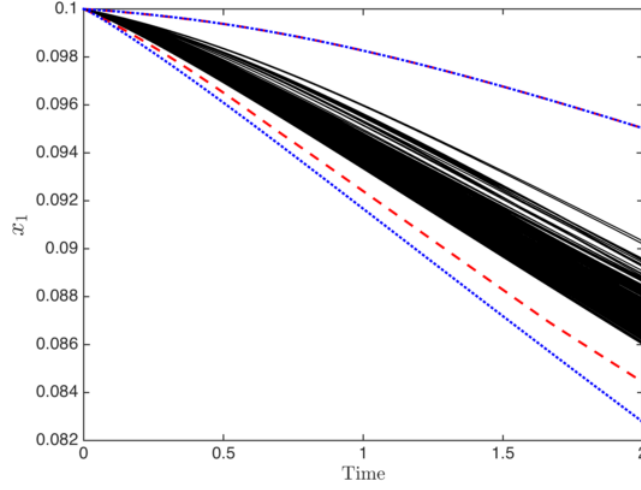


Figure 6: Comparison of state bounds on species concentration  $x_1$  from Example 2 computed using Step 8 and Step 9 in Algorithm 1. This figure demonstrates the improvements achieved by including the bound tightening operation, given in Step 9 of indirect-bounding method. Dashed red curves are the upper and lower bounding solutions with bound tightening operation included (Step 9), and dashed blue curves are the upper and lower bounding solutions with bound tightening operation excluded (Step 8). Solid curves are concentrations of the species A in the original state space computed by simulating the CSTR reaction system for constant random samples of  $\mathbf{u} = [k_1 \ u_i \ u_o]^T \in U \equiv [10, 500] \times [0.9, 1.1] \times [0.9, 1.1]$  ( $\text{M}^{-1}\text{s}^{-1}$ , liters  $\text{s}^{-1}$ , liters  $\text{s}^{-1}$ ).

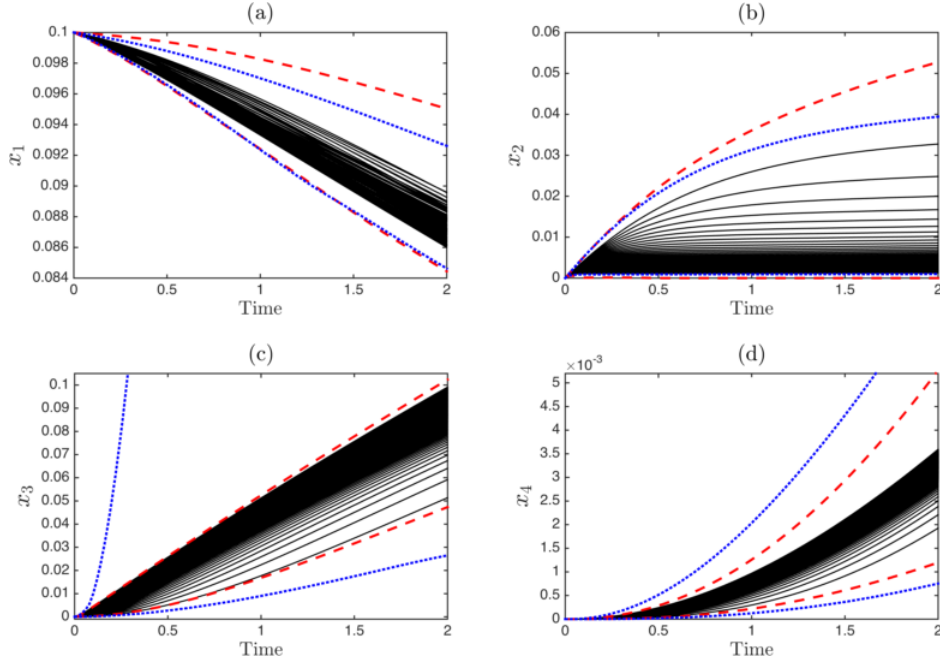
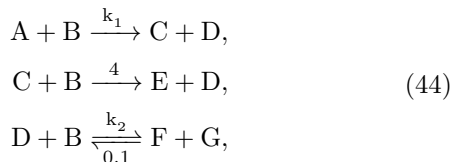


Figure 7: Comparing bounding solutions for species A through D for Example 2 obtained using direct (broken blue curves) and indirect-bounding methods (broken red curves). Bounding results for indirect-bounding method are obtained using Algorithm 2; whereas, bounding results for direct-bounding method are obtained using Algorithm 1 in [2]. Here solid curves are concentrations of the species A through D in the original state space computed by simulating the CSTR reaction system for constant random samples of  $\mathbf{u} = [k_1 \ u_i \ u_o]^T \in U \equiv [10, 500] \times [0.9, 1.1] \times [0.9, 1.1]$  ( $\text{M}^{-1}\text{s}^{-1}$ , liters  $\text{s}^{-1}$ , liters  $\text{s}^{-1}$ ).

tightening step yields a much tighter enclosure. Similar results were also observed for other states, where including the interval-tightening step yields tighter enclosures.

It is instructive to compare the bounding results from the indirect-bounding method proposed in this article with the direct-bounding method in [2]. The comparative study of the indirect and direct bounding methods for Example 1 is summarized in Figure 7, where the upper and lower bounding solutions obtained with the indirect-bounding method are represented by the red curves, while the bounding results with the direct-bounding method are represented by the blue curves. From Figures 7(a) and (b), it is clear that compared to the indirect-bounding method, direct-bounding method yields slightly tighter upper bounding solution, with no significant improvement observed in the lower bounding solution, for species A and B. Notice that the performance of the indirect-bounding method improves significantly in Figures 7(c) and (d), where it is clear that the indirect-bounding method yields much tighter lower and upper bounding solutions for species C and D compared to the direct-bounding method. The inconsistent performance of the direct-bounding method highlights a fundamental limitation with direct method discussed in Section 5 – the bounding results using the direct method strictly depend on the quality of the a priori enclosure designed for the CSTR reaction system in the original state space. While an a priori enclosure set constructed using the design proposed in [2] is efficient in reducing overestimation in species A and B, it is clearly not sufficient for species C and D. Finally, Figure 7 shows that the bounding results with the indirect method is generally tighter as compared to the results obtained using the direct method, except for species A and B, where the direct bounding method yields tighter upper bounding solutions.

**Example 3.** Consider a chemical reaction network describing ethanolysis of phthalyl chloride (A). The network includes two successive irreversible ethanolysis reactions producing desired products phthalyl chloride monoethyl ester (C) and phthalic diethyl ester (E) from ethanol (B). The reaction pair also produces hydrochloric acid (D) as a side product. It is also assumed that B reacts with D in a reversible side reaction to produce ethyl chloride (F) and water (G). Together, ethanolysis of phthalyl chloride can be described by the following chemical reaction network



in an isothermal CSTR of volume  $V = 1\text{m}^3$ . In (44), we have  $n_r = 4$  and  $n_x = 7$ . Let  $\mathbf{x} = [x_1 \ x_2 \ x_3 \ x_4 \ x_5 \ x_6 \ x_7]^T$  denote the molar concentrations of the species A, B, C, D, E, F, and G, respectively, with initial concentrations given by  $\mathbf{x}_0 = [0.2 \ 0.2 \ 0 \ 0 \ 0 \ 0 \ 0]^T$  (M). The evolution of  $\mathbf{x}$  in

the CSTR can be described by (1) with the stoichiometric matrix  $\mathbf{S}$  and rate function  $\mathbf{r}$  in (1) described by

$$\mathbf{S} = \begin{bmatrix} -1 & 0 & 0 & 0 \\ -1 & -1 & -1 & 1 \\ 1 & -1 & 0 & 0 \\ 1 & 1 & -1 & 1 \\ 0 & 1 & 0 & 0 \\ 0 & 0 & 1 & -1 \\ 0 & 0 & 1 & -1 \end{bmatrix}, \quad \mathbf{r} = \begin{bmatrix} k_1 x_1 x_2 \\ 4x_2 x_3 \\ k_2 x_2 x_4 \\ 0.1x_6 x_7 \end{bmatrix}.$$

Let the CSTR include a single input and output flow rate denoted by  $u_i$  and  $u_o$ , respectively, such that  $n_p = 1$ . Let the concentration of B in the input flow rate be 2M, such that the concentration matrix,  $\mathbf{W}$  in (1) is described by

$$\mathbf{W} = \begin{bmatrix} 0 \\ 2 \\ 0 \\ 0 \\ 0 \\ 0 \\ 0 \end{bmatrix}.$$

Given matrices  $\mathbf{S}$  and  $\mathbf{W}$ , note that the reaction network (44) only satisfies Hypotheses (2) through (3) in Theorem 2. Notice that while conditions  $\text{Rank}(\mathbf{W}) = 1 = n_p$ , and  $n_x > n_r + n_p$  are satisfied, for the stoichiometric matrix,  $\mathbf{S}$ , the rank condition is not satisfied, i.e.,  $\text{Rank}(\mathbf{S}) = 3 \neq n_r$ . A rank deficient  $\mathbf{S}$  suggests presence of a dependent reaction (see Definition 1 in [1]). This is clearly the case as evident by the presence of a reversible reaction in the network (44). Before, we can implement Algorithm 2, we need to ensure that Hypotheses (1) through (4) in Theorem 2 are satisfied. Note that using Theorem 1 in [1], we can represent the reaction network in (44) in terms of an independent network, with  $\mathbf{S}$  and  $\mathbf{r}$  redefined as

$$\mathbf{S} \equiv \begin{bmatrix} -1 & 0 & 0 \\ -1 & -1 & -1 \\ 1 & -1 & 0 \\ 1 & 1 & -1 \\ 0 & 1 & 0 \\ 0 & 0 & 1 \\ 0 & 0 & 1 \end{bmatrix}, \quad \mathbf{r} \equiv \begin{bmatrix} k_1 x_1 x_2 \\ 4x_2 x_3 \\ k_2 x_2 x_4 - 0.1x_6 x_7 \end{bmatrix}.$$

With  $\mathbf{S}$  and  $\mathbf{r}$  redefined, we have  $n_r = 3$  and  $\text{Rank}(\mathbf{S}) = n_r$ . Further, it is easy to check that Hypothesis (4) is also satisfied. In other words, the new representation of (44), satisfies Hypotheses (1) through (4) in Theorem 2.

It is assumed that  $\mathbf{x}_0$  is accurately measured, such that  $X_0 = [0.2, 0.2] \times [0.2, 0.2] \times [0, 0] \times [0, 0] \times [0, 0] \times [0, 0] \times [0, 0]$  is a degenerate interval vector in  $\mathbb{R}^7$ . Let  $\mathbf{u} = [k_1 \ k_2 \ u_i \ u_o]^T$  be a vector of uncertain variables. Assume that  $\mathbf{u}$  is restricted to the interval  $U \equiv [1, 3] \times [8, 12] \times [0.001, 0.01] \times [0.001, 0.01]$  ( $\text{M}^{-1}\text{hr}^{-1}, \text{M}^{-1}\text{hr}^{-1}, \text{m}^3\text{hr}^{-1}, \text{m}^3\text{hr}^{-1}$ ). Further, it is assumed that variation in  $u_i$  is uncertain, but always constant. Now, since  $k_1, k_2$  are the only uncertain



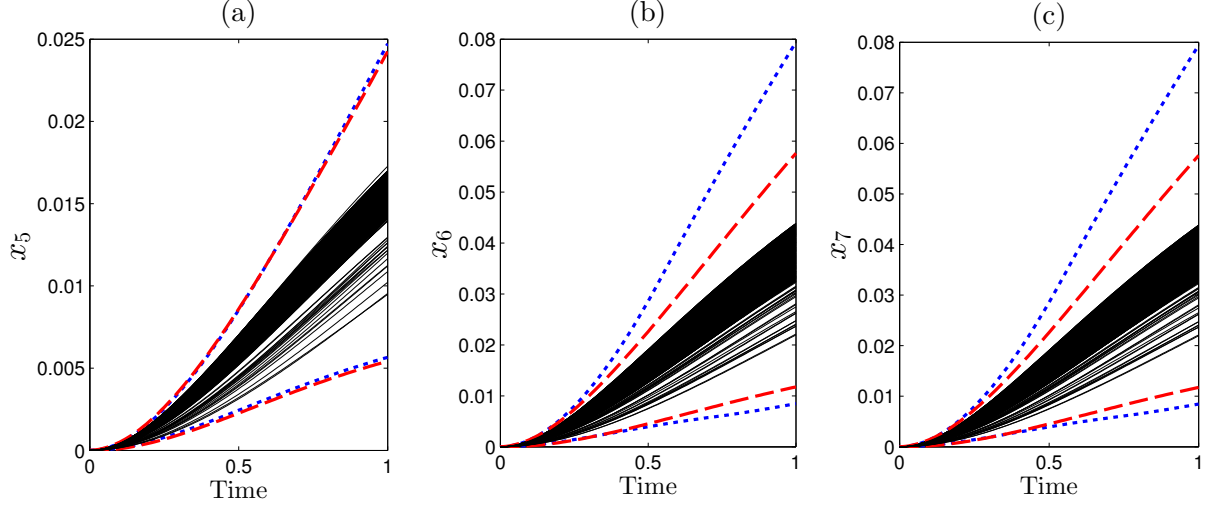


Figure 8: Comparing bounding solutions for species E through G for Example 3 obtained using direct (broken blue curves) and indirect-bounding methods (broken red curves). Bounding results for indirect-bounding method are obtained using Algorithm 2; whereas, bounding results for direct-bounding method are obtained using Algorithm 1 in [2]. Here solid curves are concentrations of the species E through G in the original state space computed by simulating the CSTR reaction system for constant random samples of  $\mathbf{u} = [k_1 \ k_2 \ u_i \ u_o]^T \in U \equiv [1, 3] \times [8, 12] \times [0.001, 0.01] \times [0.001, 0.01]$  ( $\text{M}^{-1}\text{hr}^{-1}, \text{M}^{-1}\text{hr}^{-1} \text{ m}^3\text{hr}^{-1}, \text{m}^3\text{hr}^{-1}$ ).

model parameters, we have  $n_k = 2$ . Finally, the natural bounds  $X^N = [0, 0.2] \times [0, 0.2] \times [0, 0.1] \times [0, 0.1] \times [0, 0.1] \times [0, 0.1] \times [0, 0.1]$  is given as input.

The objective is to compute interval enclosures for the reachable set of species concentration for the reaction network (44) using the indirect-bounding method outlined in Algorithm 2 over the time interval  $T = [0, 1]$ . In contrast to Example 2, the reaction system in (44) is relatively much more complicated as it involves a greater number of species and uncertain variables. For brevity, a step-by-step implementation of Algorithm 2 is not shown for Example 3; however, the results presented in this section uses the same approach as discussed in Example 2.

Figure 8 gives the upper and lower bounding solutions for species E through G computed using the indirect-bounding method (red curve). For comparison, bounding results obtained using the direct-bounding method (blue curve) in [2] are also provided along with the trajectories (black curves) for species E through G. The trajectories are computed by simulating (1) for constant random samples of  $\mathbf{u} = [k_1 \ k_2 \ u_i \ u_o]^T \in U \equiv [1, 3] \times [8, 12] \times [0.001, 0.01] \times [0.001, 0.01]$  ( $\text{M}^{-1}\text{hr}^{-1}, \text{M}^{-1}\text{hr}^{-1} \text{ m}^3\text{hr}^{-1}, \text{m}^3\text{hr}^{-1}$ ).

From Figure 8 it is clear that the indirect-bounding method yields tight enclosures for the reachable sets of species concentrations E through G. Similar results are also obtained for species A through D in the reaction network. Comparing the indirect and direct bounding methods, from Figure 8, it is clear that the indirect method yields tighter upper and lower bounds for species F and G. Further, for species A, B and E, the direct and indirect bounding methods yield similar lower and upper bounds; while, for species C and D, the direct-bounding method yields slightly tighter lower bounds (the results for

this instance is not shown for the sake of brevity). Compared to the reduction in overestimation obtained with the indirect-bounding method, the gain with the direct-bounding method for species C and D is relatively small.

Finally, as demonstrated in Examples 2 and 3, the performance of the indirect-bounding method is relatively better than the direct bounding method (see Section 5 for explanation); however, this claim cannot be generalized and extended to all CSTR reaction systems and for all the species. Any conclusive inference on the quality of bounds obtained with the direct or indirect-bounding method requires further careful analyses of the two methods, which is beyond the scope of the current paper. Based on the current work, it is not possible to gauge a priori which of the two bounding methods – direct or indirect-bounding method – yield a tighter enclosure for the reachable set of a CSTR reaction system. In such situations, it is suggested that intersecting the interval enclosures obtained with direct and indirect bounding methods for each species and at each integration time would yield the tightest enclosure. This is made possible, since the direct and indirect methods are independent and can be independently implemented in parallel for a given CSTR reaction system.

## 9. Conclusions

In this paper – the third in the three-part series – we propose an indirect-bounding method to compute interval enclosures for the reachable sets of CSTR reaction systems. The indirect-bounding method provides an alternative method to the direct-bounding method proposed in the second paper [2]. The indirect-bounding method addresses the overestimation problem inherent with the

direct-bounding method by using an isomorphic transformation, developed in the first paper [1], to map the system into a transformed state space, where enclosures are relatively simpler to compute. The interval bounds on the original states are then reconstructed using the inverse transformation. The use of indirect-bounding method also completely eliminates the need to know a tight a priori enclosure set for the CSTR reaction system, as required by the direct-bounding method. Finally, the efficacy of the indirect-bounding method was demonstrated on examples, where it was shown that the indirect method yields tight enclosures for the reachable sets of CSTR reaction systems. Further, a comparative study with the direct-bounding method highlights the reduction in overestimation with the indirect-bounding method.

## Acknowledgments

Financial support received from MIT-Novartis Center for Continuous Manufacturing is greatly acknowledged.

## References

- [1] A. Tulsyan and P. I. Barton, "Interval enclosures for reachable sets of chemical kinetic flow systems. Part 1: sparse transformation," *Chemical Engineering Science*, 2017.
- [2] —, "Interval enclosures for reachable sets of chemical kinetic flow systems. Part 2: direct-bounding method," *Chemical Engineering Science*, 2017.
- [3] M. E. Villanueva, B. Houska, and B. Chachuat, "Unified framework for the propagation of continuous-time enclosures for parametric nonlinear ODEs," *Journal of Global Optimization*, pp. 1–39, 2013.
- [4] J. P. Aubin and A. Cellina, *Differential Inclusions– Set-Valued Maps and Viability Theory*. Springer, Berlin, Germany, 1984.
- [5] A. B. Kurzhanski, "Comparison principle for equations of the Hamilton-Jacobi type in control theory," *Proceedings of the Steklov Institute of Mathematics*, vol. 253, no. 1, pp. S185–S195, 2006.
- [6] J. Lygeros, "On reachability and minimum cost optimal control," *Automatica*, vol. 40, no. 6, pp. 917–927, 2004.
- [7] I. M. Mitchell, A. M. Bayen, and C. J. Tomlin, "A time-dependent Hamilton-Jacobi formulation of reachable sets for continuous dynamic games," *IEEE Transactions on Automatic Control*, vol. 50, no. 7, pp. 947–957, 2005.
- [8] A. Chutinan and B. H. Krogh, "Verification of polyhedral-invariant hybrid automata using polygonal flow pipe approximations," in *Hybrid Systems: Computation and Control*. Springer, Berlin, Germany, 1999, pp. 76–90.
- [9] S. M. Harwood and P. I. Barton, "Efficient polyhedral enclosures for the reachable set of nonlinear control systems," *Mathematics of Control, Signals, and Systems*, vol. 28, no. 1, pp. 1–33, 2016.
- [10] A. Girard, "Reachability of uncertain linear systems using zonotopes," in *Hybrid Systems: Computation and Control*. Springer, Berlin, Germany, 2005, pp. 291–305.
- [11] A. Kurzhanski and P. Varaiya, "Reachability analysis for uncertain systems-the ellipsoidal technique," *Dynamics of Continuous Discrete and Impulsive Systems. Series B- Application Algorithms*, vol. 9, no. 3, pp. 347–368, 2002.
- [12] M. Althoff, O. Stursberg, and M. Buss, "Computing reachable sets of hybrid systems using a combination of zonotopes and polytopes," *Nonlinear Analysis: Hybrid Systems*, vol. 4, no. 2, pp. 233–249, 2010.
- [13] A. Tulsyan and P. I. Barton, "PERKS: Software for Parameter Estimation in Reaction Kinetic Systems," in *Proceedings of the 26th European Symposium on Computer Aided Process Engineering: Part A and B*, vol. 38, Portorož, Slovenia, 2016, pp. 25–30.
- [14] —, "Reachability-based fault detection method for uncertain chemical flow reactors," in *Proceedings of the 11th IFAC Symposium on Dynamics and Control of Process Systems, including Biosystems*, vol. 49, no. 7, Trondheim, Norway, 2016, pp. 1–6.
- [15] W. Walter, *Differential and Integral Inequalities*. Springer, Berlin, Germany, 1970.
- [16] V. Lakshmikantham and S. Leela, *Differential and Integral Inequalities: Theory and Applications*. Academic press, New York, USA, 1969.
- [17] J. K. Scott and P. I. Barton, "Bounds on the reachable sets of nonlinear control systems," *Automatica*, vol. 49, no. 1, pp. 93–100, 2013.
- [18] H. L. Smith, *Monotone Dynamical Systems: An Introduction to the Theory of Competitive and Cooperative systems*. American Mathematical Society, Providence, USA, 2008.
- [19] A. B. Singer and P. I. Barton, "Bounding the solutions of parameter dependent nonlinear ordinary differential equations," *SIAM Journal on Scientific Computing*, vol. 27, no. 6, pp. 2167–2182, 2006.
- [20] R. E. Moore, *Methods and Applications of Interval Analysis*. SIAM, Philadelphia, USA, 1979.
- [21] N. Ramdani, N. Meslem, and Y. Candau, "A hybrid bounding method for computing an over-approximation for the reachable set of uncertain nonlinear systems," *IEEE Transactions on Automatic Control*, vol. 54, no. 10, pp. 2352–2364, 2009.
- [22] J. K. Scott and P. I. Barton, "Tight, efficient bounds on the solutions of chemical kinetics models," *Computers & Chemical Engineering*, vol. 34, no. 5, pp. 717–731, 2010.
- [23] B. Chachuat, "MC++: A versatile library for McCormick relaxations and Taylor models," *Documentation and Source Code available at: <http://www3.imperial.ac.uk/people/b.chachuat/research>*, 2010.
- [24] S. M. Rump, *INTLAB – Interval Laboratory*. Springer, 1999.
- [25] S. D. Cohen and A. C. Hindmarsh, "CVODE, a stiff/nonstiff ODE solver in C," *Computers in Physics*, vol. 10, no. 2, pp. 138–143, 1996.
- [26] M. Amrhein, N. Bhatt, B. Srinivasan, and D. Bonvin, "Extents of reaction and flow for homogeneous reaction systems with inlet and outlet streams," *AIChE Journal*, vol. 56, no. 11, pp. 2873–2886, 2010.